



Universidade de Aveiro

2016

Departamento de Engenharia Mecânica

**Simone Schincariol**

**Otimização de nanotinta com toque metálico para componentes poliméricos da indústria automóvel**

**Optimization of nanopaint with metallic touch for polymeric auto components**



**Simone Schincariol****Otimização de nanotinta com toque metálico para componentes poliméricos da indústria automóvel****Optimization of nanopaint with metallic touch for polymeric auto components**

Trabalho apresentado no âmbito da UC Dissertação do Mestrado Integrado em Engenharia Mecânica, realizada sob a orientação científica do Professor Doutor Victor Fernando Santos Neto, professor auxiliar convidado do Departamento de Engenharia Mecânica da Universidade de Aveiro e da Doutora Maria Alexandra Lopes da Fonseca, investigadora em pós-doutoramento no Centro de Tecnologia Mecânica e Automação do Departamento de Engenharia Mecânica da Universidade de Aveiro



This work is dedicated to my family, to all the old friends and to the new ones met in the Erasmus experience.



## **o júri**

presidente

**Prof. Doutor António Completo**  
professor auxiliar do Departamento de Engenharia Mecânica da Universidade de Aveiro

**Prof. Doutor Tito da Silva Trindade**  
professor associado com agregação do Departamento de Química da Universidade de Aveiro

**Prof. Doutor Victor Fernando Santos Neto**  
professor auxiliar convidado do Departamento de Engenharia Mecânica da Universidade de Aveiro



## **agradecimentos**

Thanks to my parents and to my sister who gave me the opportunity to do the master thesis in Aveiro and thanks to my friends' support.

Thanks to all the students and the professor of Aveiro who helped, specially: Professor Doctor Victor Neto, Doctor Maria Alexandra Fonseca, Engineer Bruno Silva; from physics department Farzin Mohseni, Bruno Melo, Professor Doctor Vitor Brás Sequeira Amaral and Doctor Manuel Pedro Fernandes Graça; from ceramic department Augusto Luís Barros Lopes and Artur Sarabando. Thanks even to the University of Aveiro and the company CIE STRATIS - Tratamentos, Lda. (Varzea, Barcelos), which gave the paint and the diluent for this work.



**palavras-chave**

nanotinta, nanoparticula, componentes plásticos, industria automóvel, efeito de cromagem, condutividade térmica.

**resumo**

A cromagem de componentes para a industria automóvel é um processo que conferem prestígio aos mesmos, contudo é um processo significativamente caro, demorado e requer a adição de substratos metálicos. Esta dissertação tem como principal objetivo aumentar a sensação de toque metálico em componentes poliméricos para a industria automóvel. Desta forma, propõem-se uma alternativa ao processo de cromagem, que envolve a utilização de tinta reforçada com nanopartículas de elevada condutividade térmica. Nesta dissertação, o processo de produção de nanotintas aditivadas com nanotubos de carbono e nanoparticluas de óxido de ferro foi optimizado e a nanotinta submetida a ensaios de cor RGB, análises térmicas e elétricas.



**keywords**

nano-paint, nanoparticle, plastic component, automobile industry, chrome effect, thermal conductivity.

**abstract**

The traditional chrome plating is a process that gives prestige to car components, but it is an expensive and lengthy process that requires metal substrates. This thesis proposes an alternative to chroming process that involves the use of polymeric substrates coated with a chrome paint doped with high thermal conductivity nano-particles, in order to obtain plastic components that give the feeling of metallic touch. In this dissertation the process of production of nanopaint adding carbon nanotubes and nano- $\text{Fe}_3\text{O}_4$  has been optimized and RGB color tests, thermal analysis and electrical analysis were performed.



## Table of contents

1	Introduction.....	1
2	Literature Review .....	3
2.1	Polymers for automobile components.....	3
2.2	Chromizing parts for automobile components .....	4
2.3	Polymeric parts painting.....	8
2.4	Incorporation of nanoparticles in paint .....	10
2.5	Nanopaint health and environmental expects.....	19
3	Experimental Procedure and Results .....	27
3.1	Materials.....	27
3.1.1	Substrate.....	27
3.1.2	Paint and diluent.....	27
3.1.3	Nanoparticles .....	28
3.2	Nanopaint production procedure .....	28
3.2.1	Paint mixed with diluent – the base paint .....	28
3.2.2	Mixture of the base-paint with Carbon Nanotubes (CNTs).....	30
3.2.3	Mixture of the base-paint with the Fe <sub>3</sub> O <sub>4</sub> .....	41
3.3	Nanopaint application procedure.....	43
3.4	Experimental characterization.....	45
3.4.1	Density .....	45
3.4.2	Light reflection.....	46
3.4.3	Colour identification .....	47
3.4.4	Thickness .....	49
3.4.5	Thermal conductivity of the solid paint ( $\lambda_s$ ) .....	50
3.4.6	Thermal conductivity of the liquid paint ( $\lambda_l$ ) .....	53
3.4.7	Electrical conductivity measurements .....	54

4	Discussion of the results .....	63
4.1	Nanopaint preparation .....	63
4.2	Colour analysis .....	63
4.3	Thermal conductivity .....	65
4.4	Electrical conductivity.....	68
4.5	Health and environmental aspects.....	68
5	Conclusions and future work .....	71
5.1	Conclusions .....	71
5.2	Future work perspectives.....	72
6	References.....	75

## List of figures

<b>Figure 1.1</b> Distribution of paints and coatings' production – 2014 [1] .....	2
<b>Figure 2.1</b> Contact angle of a water droplet on a hydrophobic surface. [21].....	14
<b>Figure 2.2</b> Transparent and hydrophobic nanopaint applied on different materials: a) clay, b) wood and c) cement. [22].....	14
<b>Figure 2.3</b> FE-SEM micrographs of nano-ZnO.[27].....	16
<b>Figure 2.4</b> Fouling test over a period of 30 days. [27].....	17
<b>Figure 3.1</b> Base to apply the paint.....	27
<b>Figure 3.2</b> Original chrome paint, without diluent, mixed for 5 minutes. ....	29
<b>Figure 3.3</b> Paint <sub>200%</sub> : 50 ml of paint mixed with 100 ml of diluent. a) After 5 minutes of mixing; b) after 10 minutes; c) after 15 minutes. ....	30
<b>Figure 3.4</b> Paint <sub>200%</sub> : paint without nano-particles.....	30
<b>Figure 3.5</b> Preparation mixture of paint Sol <sub>1.1</sub> .....	33
<b>Figure 3.6</b> To the left, the surface effect of a piece painted with spray painting without CNTs, while to the right, the effect of a surface spray coating with Sol <sub>1.1</sub> . ....	34
<b>Figure 3.7</b> Above: result of the mixing of CNTs with the diluent with a magnetic stirrer after 15 minutes; below: result after 30 minutes. ....	34
<b>Figure 3.8</b> Sol <sub>2.1</sub> after 30 minutes of mixing with the magnetic stirrer.....	35
<b>Figure 3.9</b> Spray paint with mixing process Sol <sub>2.1</sub> .....	35
<b>Figure 3.10</b> Bottom of the jar with paint Sol <sub>1.2</sub> : a) 20 min, b) 30 min, c) 40 min, d) 50 min, e) 60 min, f) 70 min.....	36
<b>Figure 3.11</b> Surface irregularities caused by agglomerates of CNTs (Sol <sub>1.2</sub> ): irregularities are identified looking at the dark dots in the light gray background (bottom-right) and light dots in the dark gray background (top left). ....	37
<b>Figure 3.12</b> Bottom of the jar of paint Sol <sub>1.2</sub> while mixing manually and with ultrasonic bath: a) 10 min, b) 15 min, c) 20 min, d) 25 min. ....	38
<b>Figure 3.13</b> Agglomerates of CNTs on the stick used to mix: photo for each step of the process of ultrasonic bath and f) after cleaning.....	38
<b>Figure 3.14</b> Sediments of CNTs and/or polymeric material of the stick on the bottom of the jar....	39
<b>Figure 3.15</b> Bottom of the jar of Sol <sub>1.2</sub> , while mixing manually with the glass stick and with the ultrasonic bath: a) 5 min, b) 10 min, c) 15 min, d) 20 min, e) 25 min, f) 30 min. ....	39
<b>Figure 3.16</b> Polymeric base painted with Sol <sub>1.2</sub> .....	40

<b>Figure 3.17</b> Phase separation in the test tube of paint without nanoparticles (right) and in the one mixed with carbon nanotubes (left). ....	41
<b>Figure 3.18</b> The bottom of the jar when mixing the dye with 0,2 wt% of $\text{Fe}_3\text{O}_4$ . Left: 10 minutes. Centre: 20 minutes. Right: 30 minutes.....	42
<b>Figure 3.19</b> Polymeric base painted with $\text{Fe}_3\text{O}_4$ 0,2% .....	42
<b>Figure 3.20</b> First application of diluted paints using a common brush: 2 indicates the paint diluted to 200%, 2.5 to 250% and 3 to 300%.....	43
<b>Figure 3.21</b> Verification of the differences in painting using different instruments: in the images of the left and center was used the airbrush, in the right one we used a spray gun.....	44
<b>Figure 3.22</b> Light reflection in visible spectrum for Paint <sub>200%</sub> , CNT <sub>0,2%</sub> , $\text{Fe}_3\text{O}_4$ 0,2% and $\text{Fe}_3\text{O}_4$ 0,5%. 47	47
<b>Figure 3.23</b> Thickness measurement with the optical microscope “Nikon – Eclipse LV150” and the software “Perfect-Image V7.5”. ....	49
<b>Figure 3.24</b> Mounting the samples (yellow). ....	50
<b>Figure 3.25</b> Values of thermal conductivity varying the mass percentage of CNTs. ....	52
<b>Figure 3.26</b> Thermal conductivity for paints and nanopaints in liquid phase. ....	54
<b>Figure 3.27</b> Behaviour of $\sigma dc$ (Paint <sub>200%</sub> ) changing the temperature between 170 K to 380 K. The measurements were done for 10 V, 20 V, 30 V, 40 V and 50 V. ....	55
<b>Figure 3.28</b> I-V correlation at room temperature for Paint <sub>200%</sub> .....	56
<b>Figure 3.29</b> Behaviour of $\sigma dc$ (CNT <sub>0,1%</sub> ) changing the temperature between 230 K to 380 K. The measurements were done for 1 V.....	57
<b>Figure 3.30</b> Behaviour of $\sigma dc$ (CNT <sub>0,5%</sub> ) changing the temperature between 260 K to 380 K. The measurements were done for 0,025 V, 0,075 V and 0,1 V. ....	57
<b>Figure 3.31</b> Behaviour of $\sigma dc$ (CNT <sub>1,0%</sub> ) changing the temperature between 170 K to 380 K. The measurements were done for 0,025 V, 0,05 V and 0,075 V. ....	58
<b>Figure 3.32</b> I-V correlation at room temperature for CNT <sub>1,0%</sub> .....	59
<b>Figure 3.33</b> Behaviour of $\sigma ac$ (green triangles: Paint <sub>200%</sub> ; blue circles: CNT <sub>1,0%</sub> ) changing the temperature between 170 K to 380 K. ....	59
<b>Figure 3.34</b> Dielectric constant ( $\epsilon$ ) of Paint <sub>200%</sub> varying frequency from $10^3$ Hz to $10^6$ Hz, and varying temperature from 170 K to 380 K. ....	60
<b>Figure 3.35</b> Dielectric constant ( $\epsilon$ ) of CNT <sub>1,0%</sub> varying frequency from $10^3$ Hz to $10^6$ Hz, and varying temperature from 170 K to 380 K. ....	61
<b>Figure 3.36</b> Dielectric constant at 10000 Hz.....	62
<b>Figure 3.37</b> Dielectric constant at 100000 Hz.....	62

<b>Figure 4.1</b> Comparison of Paint <sub>200%</sub> - Fe <sub>3</sub> O <sub>4</sub> 0,2%.....	64
<b>Figure 4.2</b> Comparison of Paint <sub>200%</sub> - Fe <sub>3</sub> O <sub>4</sub> 0,5%.....	64
<b>Figure 4.3</b> Comparison of Paint <sub>200%</sub> - CNT <sub>0,2%</sub> .....	64
<b>Figure 4.4</b> Comparison of Paint <sub>200%</sub> and nanopaint. Left: Paint <sub>200%</sub> - CNT <sub>0,2%</sub> . .....	64
<b>Figure 4.5</b> Comparison of $\lambda_s$ and $\lambda_l$ for CNTs.....	66

## List of tables

<b>Table 2.1</b> Components of the GO nanopaint, and their purpose. [17] .....	11
<b>Table 2.2</b> Selected applications of nanomaterials in coatings and their functions. [18] .....	12
<b>Table 3.1</b> Chemical composition of the diluent. ....	28
<b>Table 3.2</b> Combinations with the respective variants.....	33
<b>Table 3.3</b> Nomenclature of paints and nanopaints. .....	45
<b>Table 3.4</b> Density measurements of paint diluted with 200%, 250% and 300% of diluent.....	46
<b>Table 3.5</b> Colour coordinates XYZ, Lab and RGB.....	48
<b>Table 3.6</b> Standard deviation of XYZ, Lab and RGB coordinates of Fe <sub>3</sub> O <sub>4</sub> 0,2% and av.Fe <sub>3</sub> O <sub>4</sub> 0,2%..	48
<b>Table 3.7</b> Mean and the standard deviation of Paint <sub>200%</sub> , CNT <sub>0,2%</sub> and CNT <sub>1,0%</sub> .....	49
<b>Table 3.8</b> Averages, standard deviations and uncertainties for paints and nanopaints. .....	50
<b>Table 3.9</b> Thermal conductivity, uncertainty and percentage enhancement of $\lambda_s$ .....	51
<b>Table 3.10</b> Thermal conductivity of paints and nanopaints in liquid phase with measurement's temperature and percentage variation related to Paint <sub>200%</sub> .....	53
<b>Table 4.1</b> Thermal conductivity of CNTs with different pressure. [43].....	67
<b>Table 5.1</b> Thermal conductivity of several materials. .....	72



# 1 Introduction

The main goal of the present dissertation is to study and develop an alternative method for the production of painted chrome-plated polymer parts required by the automotive industry. Nowadays the automotive industry is substituting the metal parts for the plastic ones. However, these new plastic parts must detain the aesthetic and the main properties of the metal ones, i.e., the metallic appearance is of utmost importance, as well as the “cold sensation” of metal. Those features may be obtained by the well-known chrome-plated painting. However, such method is allowed in the automotive sector even if it detains some strong drawbacks, such as the environmental aspects (the process is very toxic) as well as the economic ones (the associated costs are high).

Coatings have two primary purposes: decoration and protection. These functions are complementary in most of the paint’s usages, and about 45% of the worldwide production is intended to save and/or decorate new or existing structures, like buildings, houses and factories.

The protection and/or decoration of industrial products use 40% of the coatings. The remaining percentage covers the demand of high-performance coatings for industrial plants and equipment, vehicle refinishing, traffic paints and protection of marine structures and vessels.

The use of coating is of utmost importance in the way that its usage could improve the product’s lives, even more, coatings can prevent from degradation by environment (like acid, water, sea water, oxidation and more) or from scratches and hits. [1]

The graph shown on Figure 1.1 represents the worldwide distribution of the production of the paints and coatings. United States, Western Europe, and Japan are countries with the paint industry already mature and usually the use of paint is closely correlated with the performance of the economy in the transport and construction. Forecasts of demand for paint predicts an annual growth of 3% for the US, 2-2,5% for the European region and for only 0,5% for Japan, until 2019 since there is not a big growth in key markets such as automotive OEM (Original Equipment Manufacturer), machinery, and appliances. In emerging countries, it is expected an annual increase of the consumption more than in the developed countries.

The main core of this dissertation is the development of a new polymeric paint with metal aspect and with enhanced thermal properties, giving the plastic part a typical “cold feeling on touch” of the metallic material. A way of enhancing the thermal properties of the polymeric paint is through the addition of nanoparticles with high thermal conductivity, such as carbon-like nanoparticles (carbon nanotubes) and iron nanoparticles. It is expected that at the end of this work the main features of the

nanopaint prepared may be well understood, and the nanoparticles to be added to the polymeric base paint be identified.

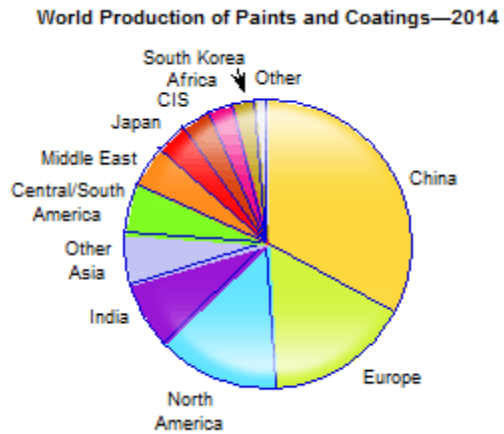


**Figure 1.1** Distribution of paints and coatings' production – 2014 [1]

## 2 Literature Review

### 2.1 Polymers for automobile components

For decades, plastics have proved to be indispensable for the automotive industry, used at first only in the cockpits or for aesthetic external components, such as mirrors, spoilers and bumpers. Today, however, plastics are also used for those components that were exclusively in metal sheet, such as doors, hoods, radiators and fenders. The almost unlimited possibilities for shaping plastics involves new experiments in design and promotes fuel economy thanks to low weight compared to metals (polymer density is about one-seventh of that of steel). Moreover, thanks to the elasticity of polymeric materials, the minor damages are reduced significantly and sometimes it is possible to easily repair them (as in the case of thermoplastics). Although in previous years the "plastic" term was associated with a poor quality material, nowadays this thought is reversing and prestigious cars confirm it. The most prestigious supercar and hypercar manufacturers are focusing increasingly on polymeric materials, or better, on composite materials: polymers enriched with particles, fibres or foils of materials that raise the properties of the compound. Pagani Zonda and Huayra, Ferrari LaFerrari, McLaren P1 and Porsche 918 Spyder are some of one million euros cars, whose chassis, bodywork and many other components are made of plastic and composite materials. Even in the most prestigious world car competition, the Formula 1, these materials represent the latest in technology and each team invests in this department. This is a demonstration of how research on automotive materials is evolving towards the polymers and their composites, able to achieve mechanical, chemical and physical properties not achievable with traditional materials.

The most widely used plastics in the automotive field are [2]:

- *PP/EPDM (Copolymer of polypropylene / ethylene-propylene-diene)*, to produce bumper and rear spoilers. Because of its non-polarity, this polymer was considered not paintable.
- *ABS (Acrylonitrile-butadiene-styrene)*, for mirrors supports, wheel covers, car roof-box accessories, front and rear spoilers. It is used in components that require good impact resistance. The acrylonitrile confers rigidity and thermal resistance (-20/80 ° C), butadiene makes the product tenacious and resistant, while styrene shall make the polymer processable. The ABS tends to become fragile and to lose elasticity when exposed to sunlight, therefore it is important to protect it against UV rays.
- *PA (Polyamide)*, is a robust and elastic material, suitable for the production of hatches for fuel tanks, but especially for wheel covers. The most used are polyamide 66 (PA66) and polyamide 6 (PA6).

- *PC (Polycarbonate)*, the high mechanical strength (even at -100 ° C) and good resistance to atmospheric agents enable that PC is suitable for the bumper and the radiator grille, which are always exposed to the weather and to collisions (example: pebbles). It is used even for lights and lenses of the front and the rear lights.
- *PU (Polyurethane)* is part of the foams and its hardness and flexibility can vary considerably, because its density increases from the center towards the surface. The core is extremely elastic, so that, after deformation, it always returns to its initial shape. PU is used to produce parts of the bumper and rear spoiler.
- *PBT (Polybutylene terephthalate)* possesses high rigidity and mechanical strength and good high temperatures, UV and wear resistances. The PBT is suitable for the manufacture of body parts such as fenders, door-handle, hood and trunk.
- *UP (Unsaturated polyester)* often is reinforced with glass fibres to increase the strength and mechanical hardness in order to compose the most extended parts of the bodywork. It is used to produce hoods, trunks, sports car fenders and components.
- *EP (Epoxy resin)* are the most used thermosetting polymers to produce advanced composites, which reach the highest performance in mechanical properties. Their processing and production often need manual labour, which greatly elevates the price of these composites and which limits their use to the luxury or competition automotive market segment.
- *PVC (Polyvinylchloride)* is very versatile since it can be produced in different variants (hard or gummy). Cover for trucks and shockproof bars can be produced with this polymer. It is used even for the manufacture of the protection of the bottom floor in the car.

Although polymers detain a set of considerable functional requirements to be used in automobile components, in the majority of the cases, it is necessary to paint this parts with different colours, being one of the most appealing one the metallic chrome aspect.

## 2.2 Chromizing parts for automobile components

The chrome plating is a well-known process that was discovered in the nineteenth century [3], used to protect metals and that nowadays can be used also in polymeric parts. The industrial chrome plating involves the use of base metallic materials on which is applied a chromium layer. It can be distinguished two processes of chrome-plating: those decorative and those with hard chromium. Decorative chromium plating is carried out to give shine and gloss, and the chromium thickness

usually does not exceed 5-8  $\mu\text{m}$ . With a thickness ranging from 8 to 250  $\mu\text{m}$ , the purpose of chromium plating in hard chrome is the protection of the metallic component, increasing the surface hardness properties (800-1000 HV), the mechanical wear resistance and the resistance to chemical attack. To obtain an aesthetic chrome plating generally it is required a nickel plating process, and sometimes copper plating, while for hard chromium only chromium is used. Chrome, nickel and copper plating are galvanic processes and before it is performed, it is necessary to clean the objects in order to remove any impurities and to remove any groove or scratch that would adversely affect the surface finish. When this part is done, it is possible to proceed with the electrolytic baths. The pieces to be treated are anchored to copper frames and connected to direct current with negative polarity (cathodes). Then, the frames are lowered into the tanks in which, in the edges, are placed a few bars of the same material to be deposited on the pieces (nickel, copper, zinc and chromium) and powered by direct current of positive sign (anodes). In those baths electro-galvanic process takes place, in which particles of the order of nanometres size are detached from the metal bars and, thanks to the magnetic polarity due to the cathode and anode, are deposited on the workpiece surface.[4][5]

If the final aim is to get the chromic-plating just for aesthetic purposes, the phase before the chromium plating, the nickel plating, generally provides a 15-20  $\mu\text{m}$  nickel deposit, for a period of 30-45 minutes (larger the nickel layer, more protects from external agents). Finally, it is proceeded with the chrome plating of the type "flash" that lasts a few tens of seconds, and allows to deposit on the surface about 5  $\mu\text{m}$  of chromium thickness. To prevent the formation of oxidation points, it is necessary, before the nickel plating, to proceed with an electrolytic bath using copper rods as anodes (copper plating). The copper plating generates a copper layer that prevents the formation of iron oxide, responsible for the oxidation points; on the other hand, this processing raises the price of the finished object. When the aesthetic appearance is overlooked, it is used the hard chrome plating process that doesn't provide for the nickel plating, since the surface hardness and the protection of the underlying material is given by the same chromium that has thicknesses reaching up to 250  $\mu\text{m}$  (0.25 mm). In order to obtain higher thickness, pieces require immersion times greater than those of the preceding case described above.[4][5]

Companies that are dedicated to chrome plating make extensive use of chromic acid (chromic anhydride)  $\text{CrO}_3$ , produced by mixing sodium dichromate and concentrated sulphuric acid. The chromium presents two forms of oxidation: the trivalent chromium Cr(III) and hexavalent chromium Cr(VI). Both are traceable in workplaces involving the use of chromium, but especially the Cr(VI) has attracted attention for its high toxicity, as to be classified as a Class I carcinogen for humans by

the International Agency for Research on Cancer (IARC) [6]. Trivalent chromium and metallic chromium Cr(0) were classified as Class III, as there are no correlations or evidence of their carcinogenicity in humans or animals. Studies on rats and mice have shown that hexavalent chromium is a source of tumours, cancer, inflammation, DNA damage [7] and other adverse consequences, as well as analysis on deaths of workers exposed to Cr (VI) have established its carcinogenicity [6]. Typically it is presented the case of an Italian company (TRICOM) in which 20 deaths were recorded: 11 for tumour and, of these, 7 for lung cancer, showing a double excess mortality for lung cancer compared to the average of the Italian population [8]. While the trivalent chromium is vital to the animal metabolism and for plants (must assimilate 0,1-0,3 mg/day), the hexavalent chromium is about 100 times more toxic. The problem lies in the fact that if the waste water is released into the environment, the salts of Cr (VI), present in them, do not precipitate in the soil and does not bind to its components. It can be moved up to aquifers that are potentially drinking water resources, causing a toxicological hazard for any animal form, and for plants [9]. There are several methods to remove the hexavalent chromium from the waste water, however, all the processes require high energy consumption or a wide use of chemical products, with the consequence of raising the costs of the chrome product [9].

An alternative to the described chromic-plating described above, is the Physical Vapour Deposition (PVD) process that can be applied to obtain thin films on substrates, by atomic or molecular deposition. The atoms or molecules derive from a liquid or solid source that is evaporated and, in the form of vapour or plasma, are transported in a vacuum chamber to condense on the substrate. For the evaporation of the condensed material various techniques are used which have in common the purpose of providing heat or energy to the material. The main methods of evaporation are: thermal evaporation; electron beam; sputtering; and arc deposition. [10]

The more practical and productive methods are arc deposited and sputtered chromium. The coating thickness that can be obtained by PVD depends on the duration time of the process: the longer it is more material will be deposited and thicker will be the coating (thicknesses of 30 microns can be achieved, in case of chromium). In addition, one can enrich the chromium with other elements, obtaining coatings like that of chromium nitride (CrN) and carbide (CrC), which do not change the aesthetic result of the chromium coating [10][11].

The substrates must have a very good surface finishing and thoroughly cleaned. The limitation of this process resides on the duration of the deposition that can reach up to 9 hours and it is highly costly (the cleaning and the equipment). Another limiting factor is the load capacity, as the vacuum chamber

has a small volume and its load capacity is directly dependent on the size and shape of the pieces to be plated, the continuous production is not possible, therefore it must be done in batches.

The positive aspects are found in the possibility of covering almost any material, which may be metals, alloys, ceramics, glasses or polymers, and in the absence of wastewater containing hexavalent chromium. For this aspect the PVD process is defined environmentally cleaned and it is a valid alternative to the galvanic processes. PVD processes allow the obtaining of high wear resistance and hardness (up to 2500-3000 HV), friction coefficient, good chemical and thermal stability, corrosion resistance and barrier to diffusion phenomena due to a coating with almost no porosity.

PVD is the process that is the closest to the electro-plating for the obtainable qualitative results and for the increase of the price of the finished component, which, in turn, is closely dependent on the quantities produced [10].

Thermal spraying can also be used to obtain the chromium finishing. The materials that can be used as coating are metals, alloys, ceramics, polymers and composites used in micrometric powder-particles fused or semi-melted. There are several process variations, such as the plasma spraying, the detonation spraying, the wire arc spraying, the flame spraying, the high velocity oxy-fuel coating spraying (HVOF) spraying warm and cold spraying [12]. The processes identified as alternatives to chrome plating and PVD coating are plasma and HVOF spray technique [10]. In the plasma spray process it is provided the use of a jet plasma, in which is inserted the powder coating that generally melts for the plasma temperatures of 15000 K. Afterwards, the fused and accelerated particles with the plasma are deposited on the substrate, adhering to it and solidifying rapidly [12].

The high velocity oxy-fuel (HVOF) spraying involves the use of a fuel-oxygen mixture consumed in a combustion chamber and the exhaust gases exit at a pressure of about 1 MPa enter into a convergent-divergent nozzle so that exceed the speed of sound, reaching about 1000 m/s. The particles of the coating are then inserted in the supersonic jet, in which they heat, ending up at a high speed on the substrate and binding to it forming a coating. [12]

Plasma process has been successful in the application of coating on steel surfaces, aluminium and magnesium, but the HVOF process turned out to be better for the layer applied, about six times lower, due to the high coating density and to the high adhesive and cohesive strength. [10]

Finally, an alternative way of chroming-plate of a part, is through polymer painting. Such technic is less costly, easier for industrial implementation and can be environmentally friendly.

## 2.3 Polymeric parts painting

As referred above, the majority of the time, plastic auto parts need to be painted for protection or for aesthetics reasons.

The painting or coating has the purpose to match the colour of the part to that of the bodywork, to obtain a brightness and brilliance the colour and, if possible, to eliminate minor production defects. An issue that cannot be ignored is the affinity of the paint with the substrate. The affinity of the paint with the plastic substrate is necessary to avoid peeling phenomena, cracking of the coatings, physical properties alteration, oxidation, depolymerization, absorption of solvents, softening and swelling of the plastic [13]. The chemical compatibility of different materials has been extensively studied, and the degree of compatibility between different substances and materials can be found [13].

The painting process involves essentially two different steps: washing/cleaning and the paint application[14] [15].

A common washing/cleaning process is the immersion of the workpiece in a water based detergent solution (or with solvents) to remove the contaminants by the chemical effect of the fluid. This process is useful if the component has complex shapes such as blind holes, indentations and undercuts. Another way of cleaning is the conjunction of the immersion with the spaying of the workpiece with a jet cleaner at high-pressure (2-20 bar). The kinetic energy of the spray, together with the effect of the detergent, removes impurities from the surface to be painted. The ultrasonic bath may be used also as a cleaning technique. The workpiece is immersed in a cleaning solution, and subjected to ultrasounds. The ultrasound, causing cavitation of the liquid, generate micro bubbles of vapour which instantly collapse on themselves, causing shock waves necessary to detach the contaminants. Dry cleaning can also be applied. In this technique direct compressed air is directed toward the workpiece in order to remove the impurities from the surface, while with the vacuum technology the contaminants are sucked. This method is suitable for the removal of chips, oil or emulsions without the use of liquids, making the procedure economical since it does not provide for the step of drying and / or cooling.

The cleaning process is of utmost importance because it eliminates the impurities that could alter the surface finish (powder and oil) and substances that do not allow a good adhesion of the paint, such as the release agents used to facilitate the extraction of the objects from the cavities of the injection moulding process.

After the cleaning process, the workpiece follows for paint application.

There are different methodologies of paint's application at industrial level, each has different characteristics and is suitable for different applications. It is also sometimes necessary the application

of a primer, the first layer of paint that can be transparent or coloured, that has the purpose of standardizing the surface on which to lay the paint. The painting process may be performed by immersion. By this process it can be identified two ways: the continuous immersion and the discontinuous immersion. In the first way, the workpieces are immersed in tanks containing the coating solution with the aid of continuous transport systems (non-stop). With this process the productivity is high, but to fill the tank it is needed an extra amount of paint by 30-50% compared to that used to coat the product. In a discontinuous immersion, the workpieces are picked up by a robot from the transport chain and immersed in the bath by vertical movement. Then they are repositioned by the robot on the conveyor chain and taken towards the oven to dry the paint. This system has lower productivity than the previous, due to its intermittence, and has a higher initial investment costs for the robotic mechanisms. It is required a careful choice of the paint and the amount of diluent to prevent dripping or accumulations of paint. [15]

Another technique of painting is by airless. Through this way the paint is sucked from a pressure pump towards the gun nozzle, where it is atomized by exploiting the nozzle divergence that does the jet expand. With this technique, air is not used to spray the paint, preventing almost completely the overspray and the high speed of application allows a reduction of time and costs of painting. These systems are generally used for anticorrosion paint applications and require pumps capable of obtaining pressures ranging from 40 to 400 bar. The control of the amount of paint must be carefully adjusted to prevent leakage at the end of painting process. [15]

Finally, the painting process can be performed by a pneumatic system. This technique uses a spray gun with the aid of compressed air. The air and the paint enter the gun by separate channels, and then join to form a uniform fan pattern. The air can be joined to the paint before or after the exit from the nozzle, it depends on the type of instrument being used, but in both cases, the paint is sprayed and dispersed from the air at high pressure. This process normally takes more than one pass to paint with the spray gun on the same spot. [15]

The paint, as referred on the standards ISO 4618; 2:53, is a material in liquid, paste or powder form, which when applied, will form a protective and decorative covering of the surfaces. It is made of complex chemical materials, which include lacquers, varnishes and other similar products. In most instances, paint is composed of the following ingredients:

- *Binders*, which is a material or product that allows connecting other materials between them. Often it is based on organic polymeric material and it ensures that the layer is coherently formed during the drying and the hardening.

- *Pigments* used as colorants, and they are usually insoluble particles.
- *Extenders* used in order to generate or change several physical properties. Most of them are mineral fillers, which are insoluble in solvents or binders.
- *Solvents*, which are individual liquids or liquid mixtures (blend) which dissolve other substances to form a solution without reacting with those substances. They may be organic such as esters, glycol ethers or aliphatic hydrocarbons, but these are going to be completely replaced by water. However, water-based paints must contain other dispersed binders.
- *Additives*, which do not have a specific composition, but are different one from each other. Usually they are added to a coating in small percentages of weight and can modify a wide range of properties such as viscosity, surface tension, gloss, structure, UV resistance and resistance to the environment.

The incorporation of nanoscale additives and the consequences, in theirs resulting properties, will be the focus of the present dissertation, in order to obtain a nanopaint close to the chrome plating.

## 2.4 Incorporation of nanoparticles in paint

The addition of nanoparticles to base materials may be translated into an enhancement of the overall properties of the based material, such as, the mechanical, thermal and electrical properties. Keeping this in mind, it can be produced a nanopaint, which can be used as a protective/decorative coating, with enhanced and interesting properties to be applied to the parts of the automotive industry, as example. But, meanwhile, it can be asked, what is exactly a nanopaint? It's a nanofluid or a nanocomposite material? Observing the preparation methodology of a nanopaint, there are similarities with a nanofluid and, before its application, the mixture is in its liquid state, but, on the other hand, after being deposited on the substrate, the nanopaint solidifies, becoming a nanocomposite. So, what is exactly a paint loaded with nanoparticles? Taking into account its final application, the nanopaint is a nanocomposite, since, once applied, it solidifies and the particles do not have freedom of movement as in a fluidic medium and the only system available to them is the diffusion through the solid medium. Furthermore, the production process of the nanopaint can be described by a production process that is used to prepare the nanocomposites. That process can be described as: 1) the paint (polymer) is mixed with a solvent (diluent) in which is added the nanoparticles; 2) the solvent is removed. In the case of the nanopaint, the solvent removal occurs through evaporation when the mixture is deposited, resulting into the solidification of the painted layer. The dosage of the diluent must be as accurate as possible, since the solidification is closely

linked to evaporation: little thinner involves rapid solidification with problems relating to cracking since the polymer chains do not have time to relax; too much diluent results in the delays into the solidification, with risks of drip and distension of uneven layer. Using water-based coating, the amount of the organic solvents is about 10/15% and that of water is about 40/50%, while, with traditional paints, the quantities of solvent are around 50/70% on the total. In our days, water-based paints are becoming increasingly widespread, as they require less organic solvents with a considerable saving of money and with a reduced environmental pollution. [16]

Table 2.1 presents an example of the composition of a Graphene Oxide (GO) nanopaint [17].

**Table 2.1** Components of the GO nanopaint, and their purpose. [17]

Additive	Material	Purpose	Weight percentage (%)
Pigment	GO sheets	Providing the color of the paint	16.0
Binder	Linseed alkyd resin	Film-forming component of paint	64.0
Stabilizer	Nano sized ZnO	Reducing the color fading effect of the paint	0.6
Anti-settling agent	Aluminum stearate	Preventing pigment and binder settling	0.5
Thickener	Thickener A	Improving the viscosity and preventing coagulation	0.1
Wetting agent	Soya lecithin	Wetting the pigment in the binder for uniform dispersion	0.6
Inner coat drier	Nano sized zirconia	Chemical cross-linking agent of unsaturated fatty acids	0.6
Outer coat drier	Cobalt napthenate	Active catalyst for the lipid autoxidation process	0.6
Thinner (solvent)	Mineral turpentine oil	Dispersing agent	17.0

Nanopaints can be prepared with a considerable number of different nanoparticles, depending on the final application of the paint. In table 2.2 are presented various functions of coatings with nanoparticles, bringing some examples and the pros and cons for each use or application area [18].

**Table 2.2** Selected applications of nanomaterials in coatings and their functions. [18]

Function	Nanomaterial (Examples)	Advantage/Effect	Industrial Branch
Color brilliance, shade, color effects (flip-flop effect), reproducible paints, easily dispersible paints	Carbon black; Oxides ( $\text{TiO}_2$ , $\text{Fe}_2\text{O}_3$ , $\text{Fe}_3\text{O}_4$ , $\text{SiO}_2$ , $\text{Cr}_2\text{O}_3$ ) (on mica flakes or $\text{SiO}_2$ spheres, with metal pigments), $\text{ZnO}$	Intensify effects of metal pigments; Stabilize pigments and fillers; Positive effects in dispersion paints; Prevent crack formation (Phyllosilicates/sheet silicates); Improve resistance to fading	Automotive, consumer goods (furniture), construction
Self-cleaning (“easy-to-clean”)	Organic-inorganic hybrid polymers (organically modified ceramics), nano-silica/ colloidal silica embedded in resin particles following polymerization; Silanes (silicon-based mixtures with other chemicals, e.g. fluorine compounds); $\text{TiO}_2$	Dirt and water repellent, Protection against algae and fungi; Anti-graffiti protection: Easy removal of unwanted paint	Automotive, construction (facades), glass
Switchable (electrochromic, photochromic, thermochromic)	Tungsten oxide ( $\text{WO}_3$ ) (electrochromic)	Color effects	Automotive
“Self-Assembly”	Polymer gel, specific organic-inorganic hybrid polymers	Self-healing surfaces	Automotive, cosmetics
Monolayer adhesive films	Polymers	Ultra-thin layers	Automotive, consumer goods
Scratch resistance	Oxide (synthetic amorphous silica), $\text{SiO}_2$ , $\text{Al}_2\text{O}_3$	Improved scratch resistance	Automotive, parquet flooring, consumer goods (furniture), optics (lenses)
Optimized flow characteristics	Oxide (synthetic amorphous silica)	Generate new rheological properties (elasticity, flow characteristics, thixotropy)	Various
Conductive coatings for electrostatic paint spraying	Carbon: Fullerenes, carbon nanotubes (CNT)	Enhanced spraying processes	Automotive

Function	Nanomaterial (Examples)	Advantage/Effect	Industrial Branch
Photocatalytic effect, antimicrobial effect	TiO <sub>2</sub> , ZnO <sup>6</sup> , Ag	Removal of grease, dirt, algae, bacteria, fungi, odorants and pollutants, transformation of NO <sub>x</sub> and ozone from the atmosphere into harmless compounds.	Construction (facades, noise barriers, tiles), road surface, vehicles, wood preservation, glass
Fire retardant	SiO <sub>2</sub>	When a certain temperature is exceeded, a heat-insulating carbon foam layer is created on the wood surface followed by a flame-resistant ceramic layer.	Construction, protection of wood against fire
Corrosion protection, wood preservation	Zinc or aluminum coated with nano-TiO <sub>2</sub> , Nano-clay (like hydrotalcite Mg <sub>4</sub> Al <sub>2</sub> (OH) <sub>12</sub> CO <sub>3</sub> xH <sub>2</sub> O)	Nano-clay coatings delay the fading of wood (which is a result of the bleeding of complex chemicals like tannins).	Construction, automotive, wood preservation
UV protection, IR reflective or IR absorbing	(TiO <sub>2</sub> ; ZnO, CeO <sub>2</sub> , iron oxide pigments (transparent iron oxide; needle- shaped particles with a length of 50-100 nm and width of 2 nm)	Enhanced UV resistance, blocking of IR and visible light, indoor climate control	Construction (facades), wood preservation, glass, plastics

A factor not to be underestimated in the production of nanoparticles is the actual and hypothetical energy savings that can consider even the production costs with today's technologies. As for the carbon nanotubes (CNTs), their production requires a considerable amount of energy, which makes the CNTs one of the materials of higher energy consumption in the world. The energy production, however, varies with the process and it is expected that in the future there will be new methods to lower energy consumption for producing such materials. [19]

The self-cleaning paints are coatings that prevent or limit the accumulation of dust and dirt, coatings added with nanoparticles like nano-TiO<sub>2</sub>, [20] which have feature applicable in various fields, such as automotive or glass industry. In fact, about glasses, if a nanocoating is applied to a glass surface, the nanoparticles will interact with UV rays, dirt will not accumulate on the glass and will be easily washed away with only the application of water. If also the paint possesses hydrophobic properties, even the water used for rinsing will not remain on the surface.

Paints with hydro and oil repellents, as well as self-cleaning, enables an increased durability of the coatings, reducing the possibility of oxidation or corrosion by external agents. To obtain these properties, it should be optimized the relationship between the surface roughness and the surface energy reduction by adding nanoparticles. By increasing the roughness of the surface, the contact angle with water and other solvents grows: that's an effect that greatly reduces the surface tension. The contact angle is the convex angle between the blue straight line and the surface shown in Figure 2.1.

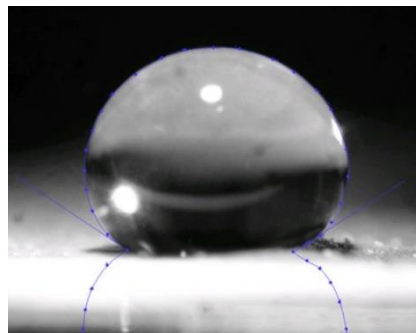


**Figure 2.1** Contact angle of a water droplet on a hydrophobic surface. [21]

When the contact angle exceeds  $90^\circ$ , the surface is defined hydrophobic, when it exceeds  $150^\circ$ , it is defined super-hydrophobic and if it reaches its maximum value of  $180^\circ$ , it will be formed on the surface a perfectly spherical droplet of liquid that ideally touch the surface at one point only. [22][21] In Figure 2.2 is shown the effects of a paint loaded with silicon dioxide ( $\text{SiO}_2$ ) nano-powders.

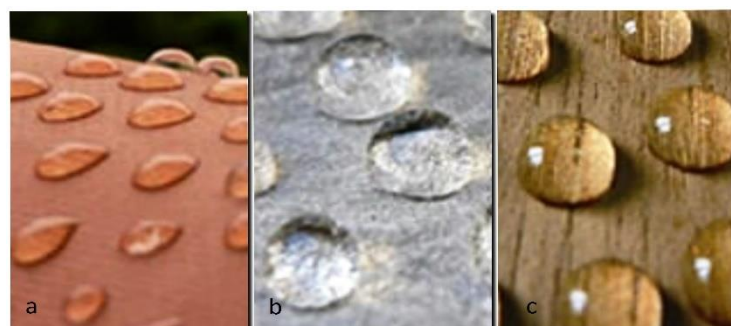


**Figure 2.2** Transparent and hydrophobic nanopaint applied on different materials: a) clay, b) wood and c) cement. [22]

Other nanoparticles have been studied to obtain nanocoating with hydrophobic characteristics, such as nano- $\text{Fe}_3\text{O}_4$ . [23] In this case different amounts of nano- $\text{Fe}_3\text{O}_4$  have been added to the paint (1 wt%, 3 wt%, 5wt%, 7 wt%) and has been measured the contact angle of a water droplet on a surface coated with such nanopaints. There has been an increased angle of contact with the increase of the

percentage of nano-oxide iron, which reached a maximum exceeding 120° for 0,5 wt%. Beyond this percentage the agglomeration process has damaged the micro-nano structure of the surface, causing a decrease in the angle of contact. With 0,5% of nano- $\text{Fe}_3\text{O}_4$  the coating is classified hydrophobic. [23]

Another major problem in esthetical coatings is due to the digital fingerprints left after touching these surfaces. To prevent this, it is possible to create an extremely flat surface with low surface free energy using the silicon dioxide ( $\text{SiO}_2$ ) nanoparticles. The fingerprints and other contaminants are reduced considerably, so areas from which begins the oxidation are limited, with a consecutive increase of piece's life.[24]

The UV rays cause photochemical degradation, which leads to oxidation and decomposition of the polymeric layers and organic or inorganic pigments. To cope with this problem may have recourse to the addition of nanopowders of oxides of titanium and zinc, which absorb and reflect harmful rays, greatly improving the UV resistance, therefore increasing durability of the coatings exposed to sunlight and to the environment. [24]

In automotive coatings based on aromatic polyurethane are often used for their good qualities against corrosion from water, acids and solvents, or for the high resistance to abrasion. However, these materials are sensitive to UV radiation, limiting factor for use on external surfaces. To obviate this problem, organic UV absorbers should be used, but these tend to move on the surface or in the substrate of the covering. Alternatively, using the 3 wt% of nanoparticles of zinc oxide, there is an absorption of UV radiation 50% greater than the film without nanoparticles, showing that the nano-ZnO can reduce the photo-degradation due to UV light.[25]

Most of the paint does not possess good scratch resistance, so they should be enriched with additives that increase such properties in order to maintain an attractive appearance for a long term and prevent the scratches become the origin of degradation phenomena of the underlying material (ex. oxidation) [24]. An example of the improvements obtainable to the scratch resistance is that of the alumina nanopowder ( $\text{Al}_2\text{O}_3$ ) dispersed in transparent and UV-curable paint with different percentages of mass of  $\text{Al}_2\text{O}_3$  from 0,2% to 2,0% [24]. Scratch resistance of these various composite coatings was measured by evaluating the loss of gloss (or blurring) due to scratches on the paints. The results were compared with the outcome obtained from the paint without  $\text{Al}_2\text{O}_3$  and has emerged that even with low percentages of  $\text{Al}_2\text{O}_3$ , scratch resistance increases by 3 to 9 times than the base material. It is possible to notice an increase of nine time on the scratch resistance by adding only 2,0% of  $\text{Al}_2\text{O}_3$  to

the original paint. These results are a clear indication of how, in general, nanopowders can lead to performance unreachable with traditional materials.

The most common flame-retardants are ammonium polyphosphate and melamine, which lose their effectiveness because of their limited mechanical performance and the reduced ability of carbonization with fire, which leads to the detachment from the substrate.

To increase the chemical and mechanical properties, fire-resistant coatings may be incorporated with nanopowders of magnesium aluminum - Layered Double Hydroxides (LDH). During the burning, these LDHs absorb heat and release water and carbon dioxide, forming a carbonized layer and lowering the temperature. [24] Other nanoparticles that can be used are the nano-TiO<sub>2</sub>.

A test with nano-TiO<sub>2</sub> was conducted to verify the actual improvement in flame retardant: the fire-resistance time is defined as the time the object tested takes to reach 300 °C when exposed to an increasing temperature flame. This test was conducted on two steel plate coated with two different flame retardant paints. The first coating contained TiO<sub>2</sub> particles of micrometric dimensions ( $40 \pm 5 \mu\text{m}$ ), the second was like the first with the addition of nano-TiO<sub>2</sub> particles ( $20 \pm 5 \text{ nm}$ ). The coating with micro-particles has reached 300 °C in 81 minutes, while the one with nanoparticles used 96 minutes, demonstrating that the addition of nano-TiO<sub>2</sub> has improved the flame resistance. [26]

The nanocoatings inhibit the adhesion of marine fouling organisms and microbes. This property is very useful for those products that are in constant contact with aggressive marine environments, as for the keels of ships or offshore structures. The nanopowders help in the reduction of germs, algae and viruses thanks to the oligodynamic effect of metal components. These innovative coatings enable to improve the performance of traditional paints and to decrease the demand for special steels such as stainless one, which has cost and time of production well above the base. An example of an alkyd resin with nanoparticles of zinc oxide (ZnO) with an average size of 100-200 nm is shown in Figure 2.3. [27]

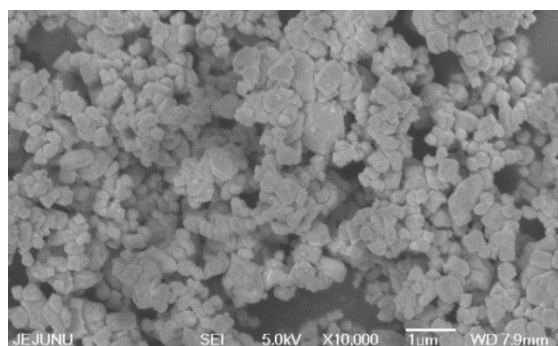
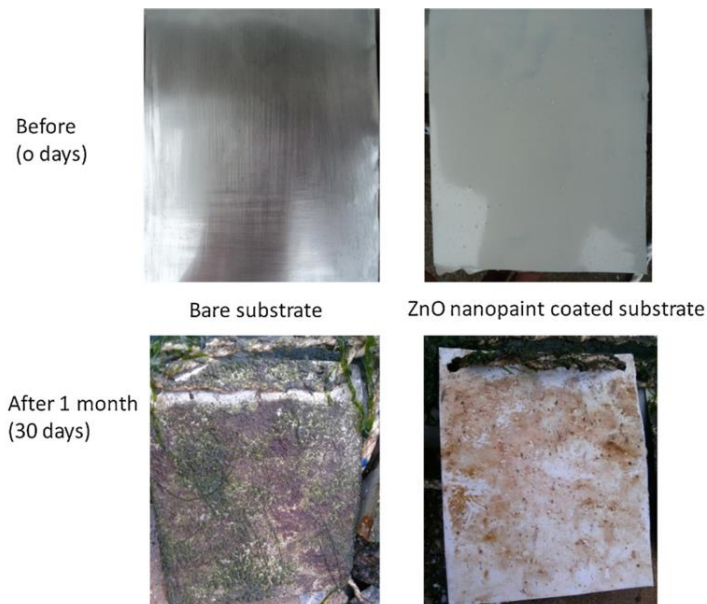


Figure 2.3 FE-SEM micrographs of nano-ZnO.[27]

To test the ability of anti-fouling, two metal plates have been used, one coated with the alkyd resin containing nano-ZnO (20 wt%), the other without coatings, and they were immersed for one month in marine water. The images of the plates before being immersed in the lagoon and after one month of exposure to salt water are presented in Figure 2.4. It can be noted how the surface with nano-ZnO is considerably cleaner than the bare one, since the antibacterial properties of the ZnO particles have inhibited the growth of marine organisms. These studies are interesting to develop products to protect keels and offshore structures, but also dams, reservoirs and wind turbines.



**Figure 2.4** Fouling test over a period of 30 days. [27]

Another property that is extremely important is related with the corrosion resistance of a paint. This is closely correlated to the ratio between the pigment and the binder (P/B), which is linked to the ability to transport corrosive and harmful elements through the coating. Coatings' anticorrosive products produce better results than traditional coatings when they reach optimum levels of nanoparticles. The nanopowders, thanks to the large surface area, are able to absorb more resin than traditional varnishes, and they are better filling the spaces between the pigments and the resin. The decrease of voids causes the paint's density increase and therefore reduces the ability to transport corrosive agents, increasing the protective properties.

One example is shown by a study on the anti-corrosive effects of titanium nanopowders (nano-Ti) with a size between 70 and 130 nm. In this case, the tests were carried out by electrochemical impedance spectroscopy (EIS) of an epoxy paint enriched with 5,0 wt%, 10,0 wt%, 20,0 wt% and on

the paint without nanoparticles. In the comparison of the diffusivity of water in the four paints, the one with the 10,0 wt% of nano-Ti has the lowest diffusivity coefficient, proving to be the best in the resistance to corrosion, as it prevents the migration of aggressive agents towards the substrate. The paint with 20,0 wt% nano-Ti is also an example of how an excess of nanoparticles is not useful or even counterproductive. [28]

Another practical example of the paint property improvements obtained with the addition of nanoparticles is suggested by a study on a nanopaint composed of epoxy resin and CNTs. The aim of this research was to analyze the increase of electrical conductivity made by carbon nanotubes. To the epoxy resin were added limited quantities of multi walled carbon nanotubes (MWCNTs) (from 0,5 wt% to 3,0 wt%) and, after the percolation threshold (1,5 wt%) were recorded values of electrical conductivity up to  $10^{-2}$  S/cm, whereas, with values less than 1,5 wt%, the electrical conductivity was about  $10^{-6}$  S/cm. Nanopaints with those values of electrical conductivity should be used as electromagnetic shielding materials. [29]

CNTs have also been used for other purposes, such as corrosion protection of carbon steel, which has been coated with an epoxy resin for this purpose. [30] The corrosion resistance of epoxy resin was compared with three nanopaint containing: 3 wt% of CNTs, 3 wt% of nano- $\text{Fe}_3\text{O}_4$  and 3 wt% of  $\text{Fe}_3\text{O}_4$ /CNTs (composite). The coating with  $\text{Fe}_3\text{O}_4$ /CNTs had the best results for corrosion protection, while the epoxy resin without nanoparticles was the worst one. Also adhesion force of the various coatings was measured, getting 0,94 MPa, 2,50 MPa, 1,77 MPa and 3,2 MPa pull-off strengths respectively for the epoxy resin, the one with 3 wt% CNTs, the one with 3 wt% nano- $\text{Fe}_3\text{O}_4$  and the one with 3 wt%  $\text{Fe}_3\text{O}_4$ /CNTs, respectively. [30]

In what concerns the production of the nanopaint, the dispersion of the nanomaterial in the paint is a critical stage, whether the nanoparticles are particulate, fibrous or lamellar. The goal is to disperse the additive uniformly in the matrix, so that every single nano-element is separated from the others. In order not to form agglomerates, the filler must be as compatible as possible with the matrix and it is necessary to use systems that enable the separation between the nano-elements. [22] The nano-dispersion methods can be categorized into high-energy or low-energy approaches. The high-energy methods usually require high pressure homogenization and ultrasound systems. Instead, the low-energy methods such spontaneous emulsification, solvent displacement and phase inversion require mechanical or magnetic mixing systems. [31] Although in the past the most used methods for the

nano-dispersion were those high energy for the approach linearity and for ease of implementation in industrial production, in more recent times the research is focused on low-energy methods. In fact, these latter processes require a lower energy consumption and less expensive equipment. However, to allow the nano-dispersion, the low-energy methods require high concentrations of surfactants which have the property of lowering the surface tension, facilitating the wettability of the surfaces or the miscibility. [31] In the high pressure homogenization systems the plant consists of a high pressure pumping system, capable of pressurizing the process fluid and force it through two break valves or homogenization in series. Here the fluid is subjected to extremely intense fluid-mechanical stress, arising by the sudden pressure drop realized and strong turbulence, which cause the break of the suspended particles into smaller fragments, up to nanometer size (nano-emulsions, nanoparticles and nano-suspensions). [32] The ultrasonic processes are used as homogenizers of the nanoparticles in the solvent. These particles may be solid or liquid. The dispersion and the breaking of the agglomerates of solids in liquids is an important application of ultrasonic devices. Ultrasonic cavitation generates high shear forces that penetrate in agglomerations by dispersing the individual particles. The mixing of powders in liquids is a common step in the formulation of various products, such as paint, ink, shampoo or beverages. The individual particles are held together by attraction forces of various physical and chemical nature, including van der Waals forces and liquid surface tension, which must be countered and overcome to break down agglomerates and disperse the particles in liquids. [33] Instead, the systems of production of nanocomposites or nanofluids at low energy require much less complex mixers of the previous two. They used mechanical and magnetic mixers (if there are no magnetic nanoparticles) useful for the homogenization of the product, while the nano-dispersion is achieved thanks to the surfactant. [31]

## 2.5 Nanopaint health and environmental expects

The expectations on nanotechnology are very high, with applicability in many fields, from industrial to medical. It is believed that with new and enhanced materials, the life of man can be extended in the future and it is placing great hopes in the reduction of environmental pollution. The preservation of the raw material, the increase of the capacity of energy storage, the reduction of greenhouse gases and energy consumption, waste water and the dispersion of potentially toxic agents in the environment are some of the purposes that may be achieve with the help of nanotechnology. [24]

Many products that include nanoparticles promise significant environmental benefits. However, it cannot be ignored the risks and potential dangers due to the special physical and chemical

characteristics of these nanopowders. Nowadays there are no evidences that these products are harmful to humans or to the environment, but ignorance in this field is still prevalent over knowledge, causing gaps especially for the safety of men and the surroundings. [34]

Some researchers are focused on the toxicity of how engineered nanoparticles (ENP) operate on cell cultures or lived organisms in controlled environments, using concentrations of nanopowder unrealistically high. The overdose of ENPs is necessary to take all side effects, although it is possible that the results deviate from those realistic. Moreover, the studies carried out on specimens will limit the analogies with natural ecosystems and the method used by the laboratory follows the one used in the chemical analysis, such as for pesticides, without considering the specific properties of nanoparticles. [34]

For analysis in the field of nanomaterials, first there is a need of tools to detect nanoparticles in the means that are gaseous, liquid or solid. Chromatography, microscopy, spectroscopy, centrifugation and filtration are some of these tools, and each can be used for different purposes, which gives different outputs: one can detect the presence of nanoparticles; the quantity or their distribution; their form or family. For each application, there is a suitable tool and often a combination of several tools is requiring having a complete analysis [35]. However, the methods that can determine the concentration and properties of nanopowders in complex environments, such as water, organisms and soil, need to be more developed.

It is not even possible to distinguish the natural nanoparticles from the artificial ones. Only isolated and targeted researches have confirmed the presence of ENPs that have entered into the environment. As for example, it has been found that nanoparticles of TiO<sub>2</sub> were washed from the surface of some layers of coatings due to rainwater effect, ending up in natural waters. [34]

The nanoparticles are not only an artificial product, but also natural and different types of nanoparticles occur in nature. The engineered nanoparticles (ENPS) are not completely identical to the natural nanoparticles as they differ in some features. The first thing to consider is the concentration: if natural nanoparticles are randomly dispersed in the environment, the artificial ones have concentration's values far beyond natural levels. The second aspect is the form of the particles: the natural powders are not considered pure, and the artificial ones have dimensions, uniform shapes and structures. Also for these differences, artificial nanoparticles are interesting by the engineering point of view, as they present unique characteristics. For example, carbon nanotubes detain high thermal conductivity and tensile strength, making them particularly attractive for technological innovative products. However, such special properties make it difficult to predict the behavior of the ENPs in the environment.

In order to determine the potential toxicity, biocompatibility is decisive: the form of the nanoparticles and its medium is detrimental because ENP's can be stable in a medium or may be removed from their disposal through agglomerations or depositions, or are transformed into forms that organisms cannot assimilate.

It can be deduced that the enormous complexity in defining the current and future risks using nanomaterials is caused by the lack of knowledge in this matter and by the wide variety of nanoparticles, each of those with its own properties and its consequences to different applications. In addition to nanoparticles characteristics' variety, other factors influence the behavior in the environment. In fact, there are different processes that take place between the nanopowders and the environment and that further vary the characteristic properties of the ENPs. Below there is a short list of those process. [36]

- *Dissolution*: nano-materials dissolve in a solvent, causing a chemical reaction.
- *Precipitation / sedimentation*: nano-materials separate from a suspension or solution.
- *Speciation*: this is a process that produces variations when nano-materials reach reaction equilibrium.
- *Formation of bonds with biotic or abiotic particles*: interaction of nanoparticles with biotic or abiotic materials (living or non-living materials).
- *Transformation*: the nanoparticles are submitted to chemical or biological changes.
- *Mineralization*: variation of a carbon nano-material containing an inorganic material, through decomposition biotic or abiotic.
- *Diffusion*: transport of nanoparticles from an environment with high concentrations to an environment with lower concentrations.
- *Deposition*: deposition of nanoparticles from one environment to another. For example, from air to water or to the ground.
- *Resuspension*: after a precipitation of nano-materials insoluble in certain liquids or gases, the nanoparticles are distributed again in the medium from which they are precipitated. For example, nano-materials are redistributed from the surface to the gas.

These processes can cause environmental changes that cannot be controlled and could not be known the consequences yet. The behavior of ENPs in different environments has been reported by a European project: [36]

- *Air.* Air is one of the optimum medium for the transport of nanoparticles for ease of movement due to air currents that distribute the particles very quickly and over long distances. Although the nanopowders spread from areas with high concentrations in areas with lower concentrations, they tend to aggregate and agglomerate when they enter into the atmosphere. Detecting nanopowder in the air is particularly difficult because the measurements of the distribution can hardly distinguish agglomerates from natural particulates. It also has not to overlook the deposition of these materials in water, in plants or in the soil, which can vary in quantity and speed because of the size of the nanoparticles (the smaller the diameter, the slower the deposition).
- *Water.* The nanoparticles in the water are presented as agglomerates of nanoparticles finely distributed in it, which behave as colloids. Water usually contains even other materials, such as natural nanoparticles, which can bind with the engineered nanopowders when added. However, the behavior of the nanoparticles is not unique in aqueous environments, but it strongly depends on factors such as salinity, pH and the presence of organic materials, that can lead to decomposition of the same ENPs and aggregates. This leads to changes in the shape and size of the nanomaterials with a consequent alteration of the physical and chemical properties of the medium. These changes can be prevented with specific materials or organic stabilizers with targeted surface modifications of the nanoparticles during their production so that they do not bind with "mutant" elements. As for the carbon nanotubes, today it is not possible to predict a behavior that is valid in every situation because the environment plays a fundamental role in the changes of their shapes, sizes and properties.
- *Soil and sediments.* Although the existence of nanomaterials has been known for decades, the researches in this field are very few, particularly regarding to their behavior in the soil and sediment. The potential toxicity of nanopowders in these areas depends on whether they bind with organic nanomaterials. For the great lack of studies in this area, we can only speculate that the transport of contaminants and ENPs in soil is not particularly significant due to their low concentrations in this environment.

Although only in recent years the nanomaterials are used and studied, it cannot be said that nanoparticles are new material. In fact, nanomaterials are present from the beginning of Earth or, even better, from the beginning of the Universe. They are materials that have been formed for various reasons, such as powders of combustion processes of volcanic eruptions or forest fires, such as

particles in almost all natural water or dust in the air obtained by the erosion of environmental agents. [34]

It is not possible to define the nanoparticles as toxic products or not, but a proper distinction according to the type of nanoparticle, to its size and to the exposure dosages is required. Some of the effects that nanoparticles have on living beings are:

- *Nano-titanium dioxide (nano-TiO<sub>2</sub>)*. Nanoparticles of titanium dioxide are one of the most interesting for industries. In fact, there are many investigations that have already led to satisfactory results on the tests carried out on algae, fish and shellfish. The peculiarity of these nanoparticles is their photocatalytic effect, which allows to act on the metabolism of the microorganisms by damaging the cell membrane. Although the effect on the ecosystem is not clarified yet, the microorganisms were particularly sensitive to nano-TiO<sub>2</sub>. By the studies conducted so far, it appears that these nanoparticles cannot damage small organisms such as shellfish, but can stick to chitinous exoskeleton of these species and prevent the suit, vital for growth, killing them. These results have been obtained with a concentration of nano-TiO<sub>2</sub> of 0,24 mg per liter of water.[36]
- *Nano-silver (nano-Ag)*. Bacteria, fungi and algae are particularly sensitive to the toxicity of the silver ions from the nano-Ag. Also the microorganisms that are found in the soil are affected by such nanoparticles. Regarding to mammals, the nano-Ag are toxic at high concentrations, indeed the US Environmental Protection Agency (EPA) has imposed 0,10 mg in one liter of drinking water and 0,01 mg per m<sup>3</sup> of air at the working place as limits of daily doses for man. While for fish and shellfish low concentrations (1 µg/l) are sufficient to obtain a negative impact on their health. The effects of such nanoparticles on the plants are not well understood, however some results point out for its damage on the cells of the growing plants. The vegetation can come in contact with these materials through the waste water that may be contaminated by washings of some particular tissues, by cleaning agents or even perfumes. [37]
- *Carbon nanotubes (CNTs)*. In the first decade after the discovery of CNTs, few studies on the its potential risks had been conducted and completed. Subsequently, thanks to new production technologies, such as Chemical Vapor Deposition (CVD) has been possible to produce CNTs in larger amounts and for industrial use. This led to conduct more studies on the environmental and toxicological risks. The results were not always unique: some researchers have determined the negative effects of CNTs, others the opposite. This resulting mismatch is due to the great variability of nanotubes, which may differ in many factors such as length, number of walls, the surface properties, the agglomerations and the structure. The similarity of the CNTs with the asbestos fibers, as regards to the form and the persistence, was the trigger for the first concerns

about the toxicity of CNTs. It is assumed that the similarity of CNTs to asbestos fibers have the same effects on the lungs and to confirm this hypothesis researchers was conducted some experiments regarding to the inhalation of CNTs by mice and rats [34]. A research has confirmed that the long (approximately 20 µm) and needle-like CNTs injected into the peritoneum led to chronic inflammation and granulomas, while there was no consequence for the short and needle-like or curved and long CNTs. Similar experiences have been conducted on mice by another researcher on single wall carbon nanotubes (SWCNTs) and on multi-walled CNTs (MWCNTs). Lung inflammation observed in mice was caused by long and rigid or thick and rigid MWCNTs, while flexible SWCNTs and thin and short MWCNTs did not compromise the health of the animals [38]. From these results, it is possible to say that the toxicity of CNTs is strictly dependent on the structural and surface properties of CNT. The longer a fiber persist deeper into the respiratory tract, the greater the likelihood that it results in harmful effects on the medium to long term (bio-persistence). It must not be forgotten that the doses of CNTs used on mice do not reflect the exposure that is normally used in everyday life. Researchers conducted experiments in guinea pigs subjected to massive concentrations to cause biological reactions and to understand the impact of such nanoparticles.

The traditional chrome plating presents a high toxicological risk for humans and a hazard for the environment during the application process of chromium. In fact, the greatest risks are incurred at the stage where the operators are exposed to the fumes of the tanks containing sodium dichromate and concentrated sulphuric acid and in the wastewater disposal stage, which, if not properly treated to remove traces of chromium hexavalent, it can spread into the environment and contaminate it. [39] However with regard to nanoparticles, as today it is known their effects, they are harmful only when plants and living beings were exposed to massive doses of ENPS (as specified previously), which greatly exceed the highest predicted exposure scenarios. [34] The hypothetical risk of contamination by nanoparticles used in nanocoatings mainly consists of three phases. 1) Production of nanocoating and application of them. 2) Release of nanoparticles in the lifetime of the coated component. 3) Dispersion of ENPS in the disposal of the component. The risks of contamination of the first stage can be greatly reduced using nano-filtering and dedicating hermetically isolated spaces systems for this process. The risk of release of ENPS during the life cycle is undetermined: it cannot exactly determine the amount of nanoparticles that are released into the environment as it is a factor influenced by the speed of degradation of the nanocoating. However, it is conceivable believe that

the nanoparticles can hardly abandon their positions, especially those at the innermost coating. In fact, they are incorporated and anchored in the polymer matrix (solid) and must be released in large quantities to be considered a hazard. [40] In the phase of the nanopaint disposal, assuming that they are disposed of in incinerators, the temperatures reached are sufficiently high to degrade a part of the nanoparticles, while the other part is present in the fumes and ashes that must be treated with systems of filtering to prevent release into the environment. [41] However, nanotechnology still has many unknown aspects, especially from an environmental and toxicology point of view, it will be necessary to move cautiously in this area, focusing on research on their toxicity and the dangers they pose.



### 3 Experimental Procedure and Results

In this chapter it will be presented and discussed the experimental procedure that was performed in these dissertation work. It will start with the materials that were user, the production of the nanopaint and its experimental characterization.

#### 3.1 Materials

##### 3.1.1 Substrate

The substrate on which the paint was applied is shown in Figure 3.1 and is made of acrylonitrile-butadiene-styrene (ABS), with dimensions of about 210x200x25 mm<sup>3</sup> and a thickness of about 2 mm. Although the substrate material has influence on the addition of the paint to it, and different surface treatments may be needed to be done in order to promote a good adhesion, for the present study it is not relevant, since the paint will be removed from the substrate to be subjected to the different analysis. However, it is worth to mention that the roughness of the substrate is not too high.



**Figure 3.1** Base to apply the paint.

##### 3.1.2 Paint and diluent

The paint and diluent were kindly provided by CIE STRATIS - Tratamentos, Lda. (Varzea, Barcelos). The commercial name of the paint and its specifications is “CELEROL®, Basecoat 990-22, Highchrome effect”. For the diluent, the commercial name is “CELEROL-Verdünner 902-82”, and its composition is listed on Table 3.1.

**Table 3.1** Chemical composition of the diluent.

Chemical name	Classification	Classification	Concentration (x)
	(67/548/CEE)	((CE) N.o 1272/2008)	
Ethyl acetate 141-78-6 205-500-4 01-2119475103-46	F; R11 Xi; R36 R66 R67	Flam. Liq. 2; H225 Eye Irrit. 2; H319 STOT SE 3; H336	40 ≤ x ≤ 100
Propanone 67-64-1 200-662-2	F; R11 Xi; R36 R66 R67	Flam. Liq. 2; H225 Eye Irrit. 2; H319 STOT SE 3; H336	25 ≤ x < 40
n-butyl acetate 123-86-4 204-658-1 01-2119485493-29	R10 R66 R67	Flam. Liq. 3; H226 STOT SE 3; H336	20 ≤ x < 25

### 3.1.3 Nanoparticles

#### 3.1.3.1 Carbon Nanotubes (CNT)

The used carbon nanotubes were purchased from “CheapTubes”. It was used multiwalled carbon nanotubes with an external diameter > 50 nm, and a length of 10-20 µm; a purity > 95 % and a density of  $\rho = 2,1 \text{ g/cm}^3$ .

#### 3.1.3.2 Nano- $\text{Fe}_3\text{O}_4$

The used iron nanoparticles were purchased to “NanoBond”, in the form of red powder. These nanoparticles have a spherical shape with a size < 30 nm and a purity of 99%. The surface area is about  $> 55 \text{ m}^2/\text{g}$  and its density is  $2,1 \text{ g/cm}^3$ .

## 3.2 Nanopaint production procedure

### 3.2.1 Paint mixed with diluent – the base paint

The paint has been shaken with a thin plastic stick to homogenize the blend, in order to not have different compositions between the top and the bottom of the tin. Several strips with different graduation of grey were still evident when stopped shaking as shown in Figure 3.2. Following this stage, a first portion was diluted in diluent. The diluent has been added in a proportion of 200%

compared to the paint, as suggested by the provider's technicians of the coating, and the doses were 50 ml of paint and 100 ml of diluent. It was used a magnetic stirrer to mix, for 15 minutes, the paint with the diluent, (evaluating the effect of the mixing every 5 minutes).



**Figure 3.2** Original chrome paint, without diluent, mixed for 5 minutes.

It was observed a clearly decrease of the viscosity of the final solution (paint + diluent), however it can be noted that some dark grey streaks were present, indicating that they are a feature of the chrome paint.

Subsequently, two other mixtures were prepared with different dosages of diluent, obtaining these three mixtures:

- Paint<sub>200%</sub>: paint 33,3% (50 ml), diluent 66,7% (100 ml)  $\frac{diluent}{paint} = 2$
- Paint<sub>250%</sub>: paint 28,6% (50 ml), diluent 71,4% (125 ml)  $\frac{diluent}{paint} = 2,5$
- Paint<sub>300%</sub>: paint 25,0% (50 ml), diluent 75,0% (150 ml)  $\frac{diluent}{paint} = 3$

The three mixtures have a viscosity that decreases as the quantity of diluent increases, but the possible variation of colour is not visible (at naked eye), or at least it is not visible before the application of the paint (Figure 3.3).

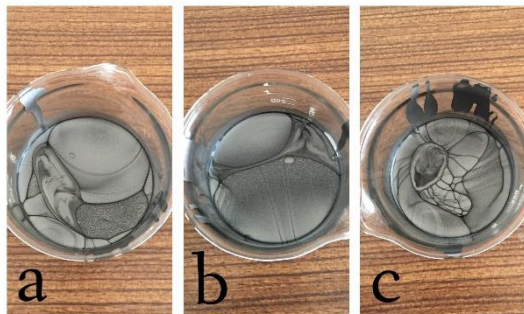


**Figure 3.3** Paint<sub>200%</sub>: 50 ml of paint mixed with 100 ml of diluent. a) After 5 minutes of mixing; b) after 10 minutes; c) after 15 minutes.

The coating of the ABS component made with a spray gun for industrial use has produced a homogeneous layer that follows the roughness and the imperfections of the substrate in ABS. At the touch it is not possible to perceive granules or agglomerates of any kind and at view the paint is brilliant. In Figure 3.4 there is a part of the piece of ABS. This paint is the reference for comparison with other types of coatings as it is the one with the doses suggested by the supplier.

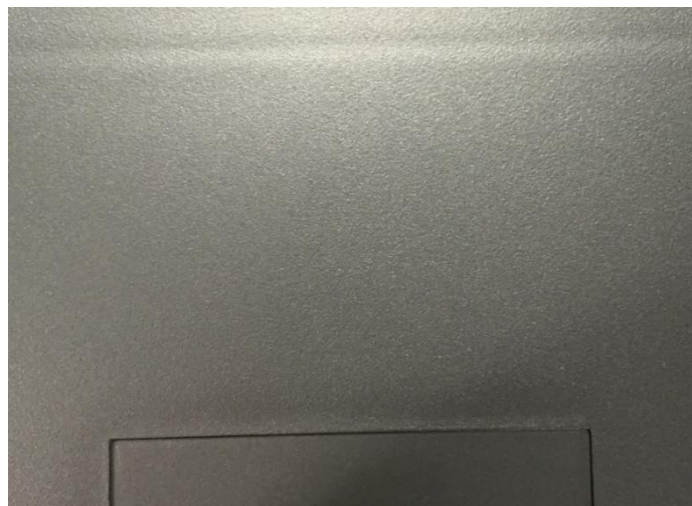


**Figure 3.4** Paint<sub>200%</sub>: paint without nano-particles.

### 3.2.2 Mixture of the base-paint with Carbon Nanotubes (CNTs)

The first nanoparticles to be used to obtain a nanocoating were the carbon nanotubes (CNTs). No functionalization treatment has been done to these nanoparticles. The nanopaints were prepared with different weight percentages of CNTs: 0,1, 0,2, 0,3, 0,4, 0,5, 0,7 and 1,0 wt% CNTs.

In order to obtain a homogeneous distribution of the CNTs into the base paint, it was optimized the way of the mixture was performed (by ultrasonic bath or using a magnetic stirrer) as well as the time of mixture.

## **Optimization of mixture time**

The optimized procedure was a combination of using first the magnetic stirrer and then the ultrasonic bath for 30 minutes.

At the initial stage of the work, the tools that were available for mixing the base paint with the CNTs were an ultrasonic tip and a magnetic stirrer. The first step was to settle up the experimental setup, and try to run the first mixture for a total mixing time of 30 minutes. It must be mentioned that the mixture could be heated due to the ultrasound and that the diluent could evaporate, so, for that reason the mixing was stopped every 5 minutes for 10 minutes to check the condition of the paint, and to ensure that there was any evaporation. The procedure that was performed is described below.

### 1) 5 minutes, ultrasonic tip

After 5 minutes of using only the ultrasonic tip, the paint was heated, but there were no noticeable decreases of the quantities of paint. Sediments of CNTs were visible, arranged radially in the bottom of the jar, indicating that the mixing had taken place only partially. To increase the mixing capacity dislodging sediments in the bottom, the ultrasonic tip was combined with the magnetic stirrer. Before proceeding with the second part of the mixing, the paint was left to cooldown for about 10 minutes

### 2) 5 minutes, ultrasonic tip + magnetic stirrer

In the bottom of the jar, there were no sediments, but the paint was still hot. The colour of the painting did not visibly change from the original colour, but only after the application you can be assured that there have been no changes. After an hour and a half, sediments were still visible in the bottom of the jar, but far fewer than in the first step.

### 3) 5 minutes, ultrasonic tip + magnetic stirrer

There were no sediments at the bottom, the paint was heated and the colour was apparently unchanged. To speed the cooling and to disperse the heat absorbed by the paint, the jar was placed in a larger bowl containing water at room temperature, using the system in a water bath, till the temperature of the paint has fallen.

### 4) 5 minutes, ultrasonic tip + magnetic stirrer + water bath

After these 5 minutes, the paint does not present residues at the bottom, the colour was unchanged and its temperature was not increased. Therefore, it was decided to lengthen the mixing time thanks to the bain-marie system.

5) 10 minutes, ultrasonic tip + magnetic stirrer + water bath

After 10 minutes, the mixture appeared homogeneous and without residues, without colour changes and its temperature was slightly higher than room temperature, but not significant.

A total mixture time of 30 minutes was achieved and the paint was preserved in a test tube to check the possible formation of sediment in the bottom.

As the time of mixture were optimized, for other mixings, it was adopted the system in a water bath to postpone the control steps at 15 minutes and to decrease the temperature, with the combination of the ultrasonic tip and the magnetic stirrer to increase the mixing capacity, for a total mixing time of 30 minutes.

### **Optimization of the mixture**

It was optimized the mixture itself, or check which mixing process to follow, considering also that the methodology should be applied in the industry (it must be simple with easy implementation).

1) Preparation of the paint.

To prepare the paint four different were followed paths using the same dosages, in order to understand which of the procedures could lead to a more homogeneous mixture. Among the various procedures, the order of mixing and the type of applied mixer were changed.

### **ORDER OF MIXING**

- Sol<sub>1</sub>: paint + diluent → (paint + diluent) + CNTs
- Sol<sub>2</sub>: diluent + CNTs → (diluent + CNTs) + paint

### **MIXER**

- Mix<sub>1</sub>: magnetic stirrer
- Mix<sub>2</sub>: ultrasonic bath

Table 3.2 shows the four combinations with the respective variants:

**Table 3.2** Combinations with the respective variants.

	Mix1	Mix2
Sol1	Sol <sub>1.1</sub>	Sol <sub>1.2</sub>
Sol2	Sol <sub>2.1</sub>	Sol <sub>2.2</sub>

The base paint (paint + diluent) was previously prepared. For the Sol<sub>1.1</sub>, a weight percentage of 0,2 % CNTs was added to the into the mixture. The mixing started with a magnetic stirrer for 30 minutes with a control step each of 15 minutes. Figure 3.5 shows a photograph of the mixture Sol<sub>1.1</sub> after 30 minutes of mixing, agglomerates of CNTs were not visible.



**Figure 3.5** Preparation mixture of paint Sol<sub>1.1</sub>.

Figure 3.6 shows a comparison of the results of the painting with Sol<sub>1.1</sub> with the result of the painting without CNTs. It can be seen in the left image (the painting without CNTs) that surface finish is much less erratic than that of the right with CNTs (Sol<sub>1.1</sub>). The surface of the right is much rougher than the other, in fact, the carbon nanotubes, when stirred, did not disperse in the mixture of paint as hoped, but it came together in clusters that form in the paint visible bumps in photo. This roughness also tends to change the paint color, because the protuberances generate tiny light and shadow effects, which vary the appearance of the object painted.

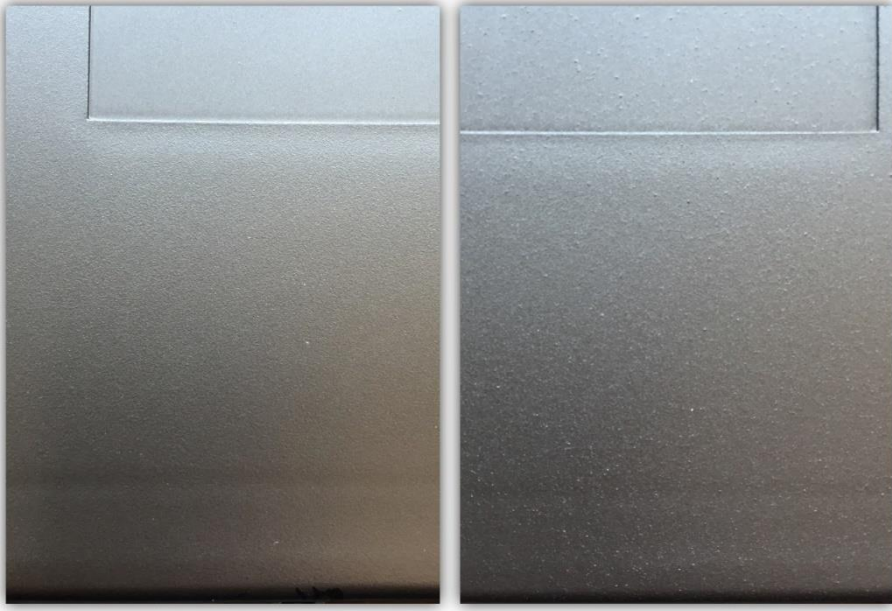


**Figure 3.6** To the left, the surface effect of a piece painted with spray painting without CNTs, while to the right, the effect of a surface spray coating with Sol<sub>1.1</sub>.

For Sol<sub>1.2</sub> it was changed the the mixing process applied to Sol<sub>1.1</sub>. The CNTs were mixed with the diluent before mixing it with the paint.

The CNTs were mixed with the diluent with a magnetic stirrer for a total of 30 minutes with a verification check each 15 minutes. Figure 3.7 shows the results of the final mixing after 15 minutes and after 30 minutes.

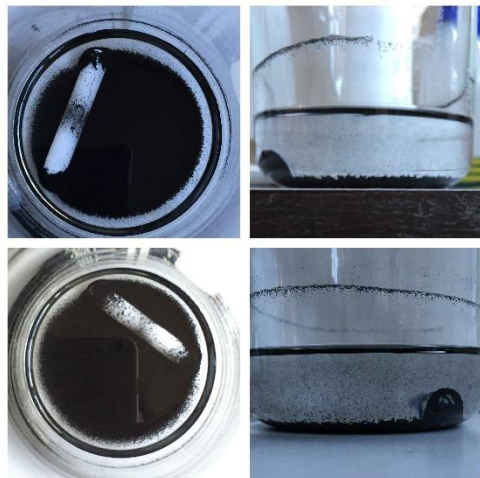


**Figure 3.7** Above: result of the mixing of CNTs with the diluent with a magnetic stirrer after 15 minutes; below: result after 30 minutes.

As it can be seen, the mixing of the diluent with the CNTs was not successful; in fact, the CNTs are not completely dispersed in the diluent and it is clearly visible some sedimentation of the CNTs on the bottom of the glass jar. This result suggests that CNTs are not soluble into the used diluent for this coating. After mixing the CNTs with the diluent, the paint was added. Such mixture was mixed for 30 minutes through a magnetic stirrer. The obtained mixture can be seen in Figure 3.8. It can be noticed that on the right picture it appears some dark gray spots in the bottom of the jar, indicating possible agglomerates of CNTs.

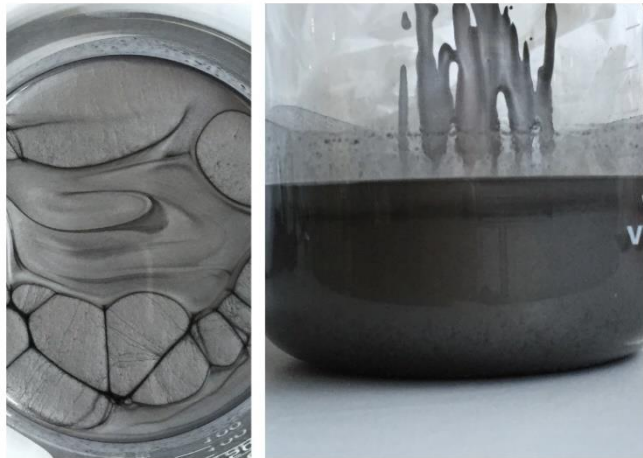


**Figure 3.8** Sol<sub>2,1</sub> after 30 minutes of mixing with the magnetic stirrer.

In this case, after painting, the results obtained do not differ much from those of Sol<sub>1,1</sub>, in fact, as seen in Figure 3.9, there are obvious protuberances that make the surface very rough.

This roughness is due, as in the previous case, to agglomeration of CNTs.

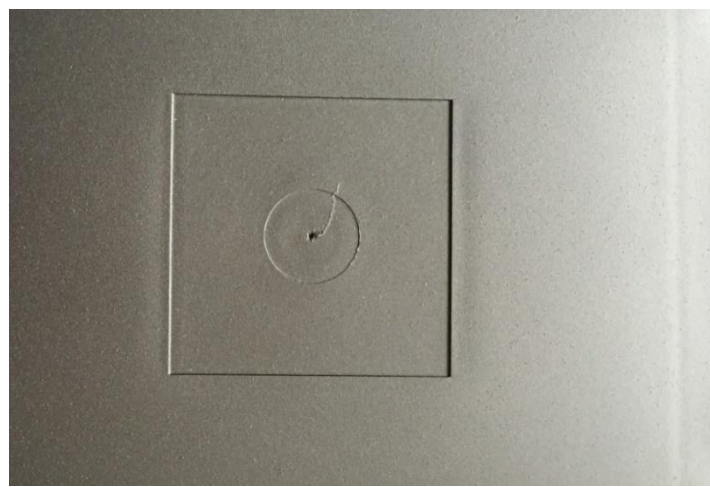


**Figure 3.9** Spray paint with mixing process Sol<sub>2,1</sub>.

From the results of this and the previous coatings, it can be assumed that the mechanical mixing is not the most suitable solution to obtain a uniform paint and with a good surface finish. That is not a

process sufficient to obtain a dispersion of nanoparticles that allows obtaining satisfactory results at the sight and to the touch. In addition, the mixing of CNTs with the diluent, before adding the chrome tint, has not yielded positive results as you can see in the picture of Figure 3.7, so it was decided not to proceed with Sol2.2 solution, knowing that the CNTs do not disperse in only thinner. Therefore, it was necessary to continue with the tests using Sol<sub>1.2</sub>.

Before proceeding with Sol<sub>1.2</sub>, the CNTs were placed in an oven, for 5 hours, at 100°C and 0% of humidity, in order to remove the possible excess of humidity. Through this process it was possible to reduce the humidity of the CNTs and enable a better solubility in the paint, since it was verified that the paint was not compatible with water.

To proceed with the Sol<sub>1.2</sub> the CNTs were added to the mixture, and it was used an ultrasonic bath for a total of 70 minutes (20-10-10-10-10-10). Figure 3.10 shows the photographs of the bottom of the jar containing the paint at each step.

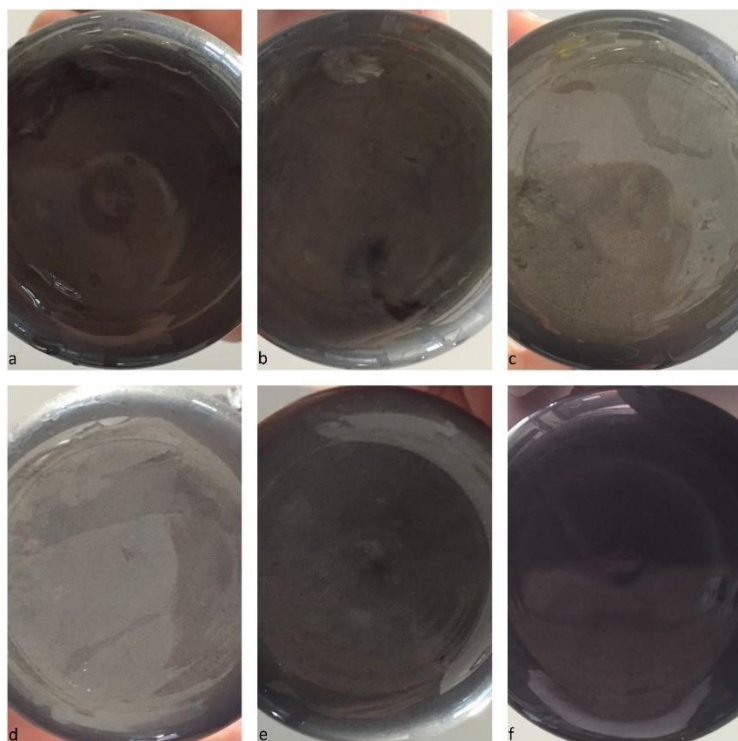


**Figure 3.10** Bottom of the jar with paint Sol<sub>1.2</sub>: a) 20 min, b) 30 min, c) 40 min, d) 50 min, e) 60 min, f) 70 min.

As it can be seen, after 40 minutes, there are some visible traces of CNTs (images a, b, c), thereon the agglomerates of CNTs could not be noted on the bottom of the jar. As a precaution, the mixing in ultrasonic bath was conducted for a total of 70 minutes, in order to disperse the agglomerates of

CNTs, even if not visible. Then we proceeded with the painting of a piece of plastic with the mixture Sol<sub>1.2</sub>, achieving a significantly better result than Sol<sub>1.1</sub> and Sol<sub>2.1</sub>.

Figure 3.11 shows a part of the painted substrate, in which it can be noticed some surface irregularities that alter the final finish compared to the paint without nanoparticles. These irregularities are much less numerous than the two previous cases, in fact, the roughness and the matting effect is less. However, we have not achieved satisfactory effects to the eye and touch yet, we must then reduce the number and size of the agglomerates of CNTs to avoid bumps and surface imperfections.



**Figure 3.11** Surface irregularities caused by agglomerates of CNTs (Sol<sub>1.2</sub>): irregularities are identified looking at the dark dots in the light gray background (bottom-right) and light dots in the dark gray background (top left).

It was prepared again Sol<sub>1.2</sub> with manual mixture of the 0,2 wt% CNTs. To improve the mixing, a stick of polymeric material was used for manual mixing, while the mixture is subjected to the ultrasonic bath. This procedure was adopted to increase the speed of dispersion of the CNTs, as it was believed that manually shaking the mixture agglomerations would break more easily and quickly.

Such “assisted” mixture was performed for a total of 25 minutes (with intervals at 10, 15, 20, 25 minutes), changing the water of the tank of the ultrasonic bath to each step, to maintain temperature of the paint low (room temperature).

In Figure 3.12 there are some pictures of the bottom of the jar at each interval and it can be seen that there are no agglomeration, even for 10 minutes of mixture.

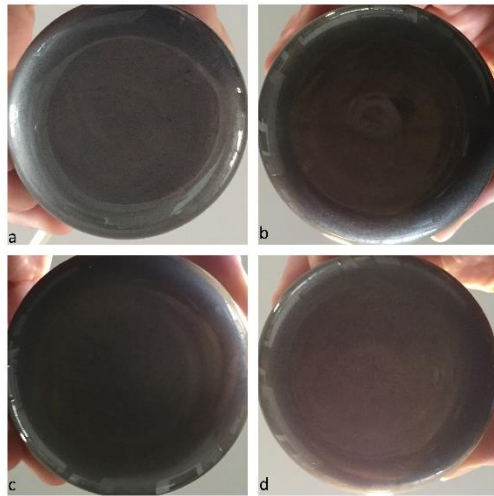


**Figure 3.12** Bottom of the jar of paint Sol1.2 while mixing manually and with ultrasonic bath: a) 10 min, b) 15 min, c) 20 min, d) 25 min.

The mixing was stopped after 25 minutes because the carbon nanotubes agglomerated and attached to the plastic stick (Figure 3.13).

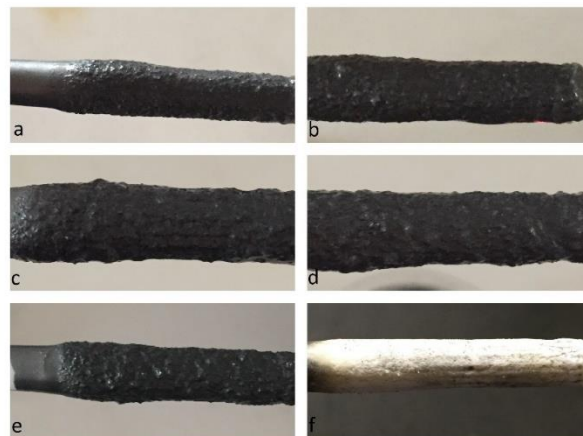


**Figure 3.13** Agglomerates of CNTs on the stick used to mix: photo for each step of the process of ultrasonic bath and f) after cleaning.

It was possible that the stick had attracted the CNTs due to an electrostatic effect, then we tried to disperse CNTs leaving the stick immersed in the mixture with the ultrasonic bath. The process continued for 25 minutes without positive effects because the agglomeration didn't come off the stick, therefore we decided to discard this paint sample and not to proceed with painting because the doses of CNTs would have been altered. During the cleaning of equipment, it was discovered that, in the bottom of the jar, sediment remained with different texture from that one of the paint. The stick had

been affected, maybe by the chemical effect of the diluent, combined to the physical effect of ultrasound, and had lost the original shape and texture (Figure 3.13.f). Probably the sediments remained on the bottom of the jar (Figure 3.14) were not only agglomerations of CNTs, but also particles of polymeric material of the stick. Also for this reason, the sample of chrome paint was unusable.



**Figure 3.14** Sediments of CNTs and/or polymeric material of the stick on the bottom of the jar.

This sample was discarded and a second one was prepared, using a glass rod stick.

The total time of mixing of this new sample was 30 minutes, with steps of 5 minutes to change the water of the bath and took some photos of the bottom of the jar (Figure 3.15). It can be noted that, since the first five minutes, there are no agglomerates of CNTs at naked eye and the stick was not affected by the diluent and had not attracted CNTs by electrostatic effect.



**Figure 3.15** Bottom of the jar of Sol<sub>1.2</sub>, while mixing manually with the glass stick and with the ultrasonic bath: a) 5 min, b) 10 min, c) 15 min, d) 20 min, e) 25 min, f) 30 min.

After mixing, it was proceeded with the drafting of the first layer of paint. As it will be explained later, to proceed with the drafting of the second layer we have waited 15 minutes for the first to dry enough to catch the second. During the 15 minutes of drying, the paint was subjected to manual mixing and ultrasonic bath for 10 minutes, so that there were not any agglomerates fallen to the bottom of the vessel. The coating is shown in Figure 3.16.



**Figure 3.16** Polymeric base painted with Sol<sub>1.2</sub>.

Touching this painting, it is possible to feel the roughness, indicating that the dispersion of the agglomerates was not enough to make acceptable surface finish. At the sight, the piece of plastic is slightly less shiny than that one painted without CNTs, but it is the sample that proves less roughness to the touch and shows fewer imperfections at the sight.

To get further indication on the quality of mixing, it was prepared a test tube containing nanopaint and using Sol<sub>1.2</sub> procedure with 0.2 wt% of CNTs. The purpose was to verify possible phase separation and potential sedimentation of carbon nanotube agglomerates.

The test tube exhibited a distinct division of colours that suggests a separation of phases. In Figure 3.17 (right figure) it is possible to note how the upper part of the tube is of a light grey colour, while the lower part is darker and, after careful observation, dark grey granules are noticed, which in fact alter the colour of the lower part.

As a first hypothesis for this effect, it can be said that the mixing was not distributed because the nanotubes were concentrated in the lower part after a day of rest. The carbon nanotubes have a higher density than the diluted paint, which allowed the separation of the stages vertically. Looking at only the bottom, one could say that the mixing was well distributed, but not much dispersed, because it seemed that nanotubes had formed small but visible grains of nanotubes, which are still too large compared to the nanoscale.

However, a second test tube was filled with paint diluted to 200% without nanoparticles (Figure 3.17 to the left), to compare the results that would be obtained leaving both paints to rest. In the following days also in the test tube containing the paint without nanoparticles a vertically phase separation has occurred. This suggested that the cause of this division were not nanoparticles as originally thought, but it was the thinner, which, if left to rest, will separates from the paint and tends to evaporate.

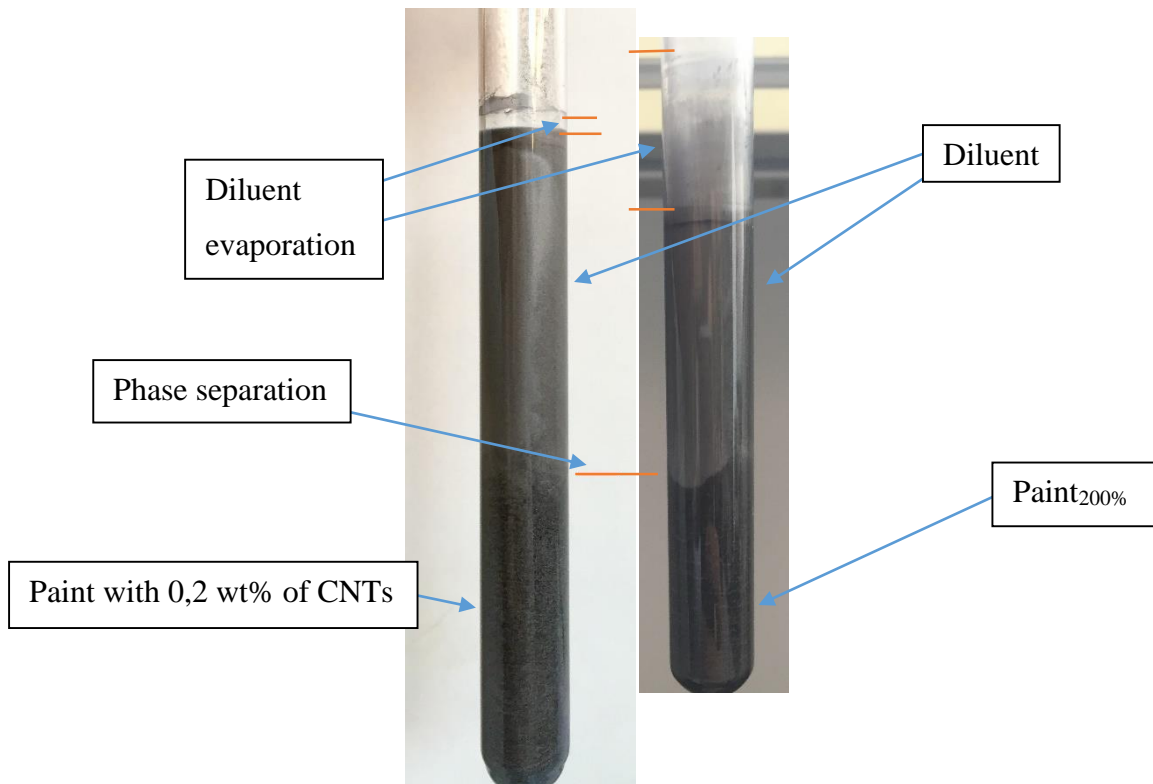


**Figure 3.17** Phase separation in the test tube of paint without nanoparticles (right) and in the one mixed with carbon nanotubes (left).

### 3.2.3 Mixture of the base-paint with the $\text{Fe}_3\text{O}_4$

After optimizing the procedure of how to prepare the nanopaints with CNTs, iron oxide nanoparticles ( $\text{Fe}_3\text{O}_4$ ) were also tested. The samples were prepared with 0,2 wt% of  $\text{Fe}_3\text{O}_4$ . The first mixture was prepared as the same of Sol<sub>1,2</sub>:

$$(\text{paint} + \text{diluent}) + \text{Fe}_3\text{O}_4$$

The procedure was performed with the ultrasonic bath simultaneously with the manual mixing with a glass rod, stopping the mixing every 10 minutes to check the overheating and to change the water of ultrasonic bath. A total mixing time of 30 minutes was used. In Figure 3.18 there are some pictures of the bottom of the jar to check if there was some sedimentation of the  $\text{Fe}_3\text{O}_4$ .



**Figure 3.18** The bottom of the jar when mixing the dye with 0,2 wt% of  $\text{Fe}_3\text{O}_4$ .  
Left: 10 minutes. Centre: 20 minutes. Right: 30 minutes.

$\text{Fe}_3\text{O}_4$  0,2% is the paint with 0,2 wt% of iron oxide. It can be noted from a photographic comparison as this mixture (Figure 3.19) will present less erratic than the one containing CNTs (Figure 3.16).

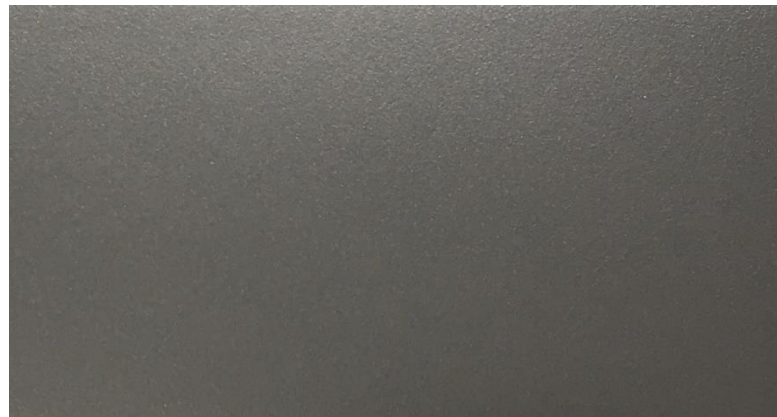


**Figure 3.19** Polymeric base painted with  $\text{Fe}_3\text{O}_4$  0,2%.

This difference is found also to the touch, in fact, the roughness of  $\text{Fe}_3\text{O}_4$  0,2% is less than that one of CNT<sub>0,2%</sub>. This result might be attributed to the different size and shape of the nano-iron oxide particles, which measure not more than 30 nm and which have a spherical shape. Instead the carbon nanotubes have a cylindrical shape and tend to tangle with each other making it difficult their separation. As well as the intermolecular forces may be greater in the case of CNTs, which would not allow a sufficient separation of the nanoparticles that are grouped forming agglomerates. Another factor that may affect this result can be the difference in volumetric proportion of the two types of nanoparticles having different densities: the volume occupied by the nano- $\text{Fe}_3\text{O}_4$  is less than that of CNTs, which would allow a dispersion of nanoparticles more effective for the iron oxide.

To verify the actual nano-dispersion improvement obtained with the mixing of the iron oxide nanoparticles, it was prepared a solution containing the 0,5wt% of nano- $\text{Fe}_3\text{O}_4$  ( $\text{Fe}_3\text{O}_4$  0,5%), corresponding approximately to the same CNT<sub>0,2%</sub> volumetric percentage.

In this case the coating is darker than Paint<sub>200%</sub>, Fe<sub>3</sub>O<sub>4</sub> 0,2% and CNT<sub>0,2%</sub>. However, touching it, it seems to be less rough than the paint with CNTs. Its low roughness should be caused by the shape and the dimension of the nanoparticles, but not by the volumetric percentage. In fact, this sample has about the same volumetric quantity of nano-powder like the CNT's paint.

For the measurement of the thermal conductivity in liquid phase was prepared even a nanopaint with 0,1wt% of nano-Fe<sub>3</sub>O<sub>4</sub> (Fe<sub>3</sub>O<sub>4</sub> 1,0%).

### 3.3 Nanopaint application procedure

For the first application of the paint in the ABS workpiece, it was used an ordinary brush, but it was a poor choice. The paint strokes were not comparable to notice any color changes due to different amounts of diluent as the drafting could not be defined uniformly, as shown in Figure 3.20. According to the brushstroke, it was changed the amount of deposited material, the thickness of the layer, the gloss and its uniformity. To limit the uncertainty due to the operator and due to the painting tools, two airbrush was tested and used.



**Figure 3.20** First application of diluted paints using a common brush: 2 indicates the paint diluted to 200%, 2.5 to 250% and 3 to 300%.

The best airbrush was a spray gun with cup, Einhell, art.-Nr 41.330.00. For the first test, it was used the paint with the ratio diluent/paint equal to 2, to check if the deposition of the layer was homogeneous. The results obtained were satisfactory, as showed in Figure 3.21.

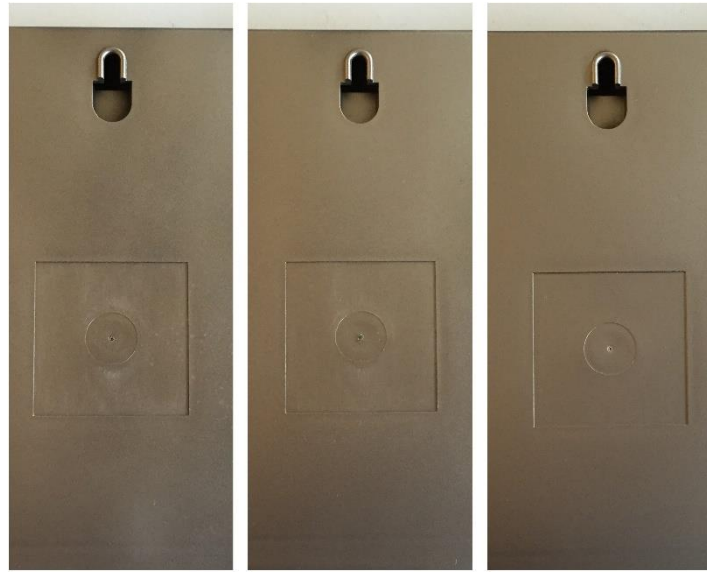


**Figure 3.21** Verification of the differences in painting using different instruments: in the images of the left and center was used the airbrush, in the right one we used a spray gun.

To obtain the painted specimens with only one type of coating, it was followed the procedure below:

- Clean the surface of the ABS component with ethyl alcohol
- Application of the coating (2 applications)
- Drying (2 days)
- Cutting the coated component in a smaller size
- Peel off the paint from the ABS substrate

To obtain the specimens with two types of coatings (side by side to compare colour at naked eye), it was followed the procedure below:

- Cut the ABS component in a smaller size
- Clean the surface with ethyl alcohol
- Partial coverage of the specimen with a paper scotch tape
- Application of the first type of coating (2 applications)
- Drying (two days) and tape removal
- Coverage of the painted surface with a foil of aluminium
- Application of the second type of paint (2 applications)
- Drying (two days) and removal of the aluminium foil

In order to obtain adequate thicknesses of the layers for the measurement of the thermal conductivity (at least 25 µm), it was necessary to proceed with 4 applications of paint.

### 3.4 Experimental characterization

Different experimental techniques to characterize the prepared nanopaints (with CNTs and Fe<sub>3</sub>O<sub>4</sub>), as well as the base paint, have been carried.

Table 3.3 lists the different types of paint and nanopaint produced and tested, indicating the respective volumetric percentage of diluent and the weight percentage of nanoparticles.

**Table 3.3** Nomenclature of paints and nanopaints.

Name	Diluent vol%	Nanoparticles	Nanoparticles wt%
Paint <sub>0%</sub>	0	None	0
Paint <sub>200%</sub>	200	None	0
Paint <sub>250%</sub>	250	None	0
Paint <sub>300%</sub>	300	None	0
CNT <sub>0,1%</sub>	200	CNTs	0,1
CNT <sub>0,2%</sub>	200	CNTs	0,2
CNT <sub>0,3%</sub>	200	CNTs	0,3
CNT <sub>0,4%</sub>	200	CNTs	0,4
CNT <sub>0,5%</sub>	200	CNTs	0,5
CNT <sub>0,7%</sub>	200	CNTs	0,7
CNT <sub>1,0%</sub>	200	CNTs	1,0
Fe <sub>3</sub> O <sub>4</sub> 0,2%	200	Nano- Fe <sub>3</sub> O <sub>4</sub>	0,2
Fe <sub>3</sub> O <sub>4</sub> 0,5%	200	Nano- Fe <sub>3</sub> O <sub>4</sub>	0,5
Fe <sub>3</sub> O <sub>4</sub> 1,0%	200	Nano- Fe <sub>3</sub> O <sub>4</sub>	1,0

#### 3.4.1 Density

In order to dose with more precision, it was necessary to know the density of the materials that were going to be used: paint and nanoparticles (CNTs and Fe<sub>3</sub>O<sub>4</sub>). The density of the nanoparticles was provided by the companies. However, the density of the paint was not well known, in such way that the paint was diluted with different amounts of diluent (200%, 250% and 300% of diluent), and so, with different densities. The density was measure with a densimeter Digital Density Meter Model DDM 2910 by Rudolph Research.

Five measurements were completed for each of the three paints and the average and the standard deviation of the obtained results were calculated. The results are summarized in Table 3.4.

**Table 3.4** Density measurements of paint diluted with 200%, 250% and 300% of diluent.

# of measurement	$\rho_{200\%}$ [g/cm <sup>3</sup> ]	$\rho_{250\%}$ [g/cm <sup>3</sup> ]	$\rho_{300\%}$ [g/cm <sup>3</sup> ]
<b>1</b>	0,8783	0,8669	0,8633
<b>2</b>	0,8783	0,8669	0,8633
<b>3</b>	0,8782	0,8668	0,8633
<b>4</b>	0,8781	0,8668	0,8632
<b>5</b>	0,8781	0,8668	0,8632
<b>Mean</b>	0,8782	0,8668	0,8633
<b>SD</b>	0,0001	0,0001	0,0001

As it can be seen, the density decreases with the enhancement of the diluent contents, as it was expected.

### 3.4.2 Light reflection

In order to identify the variations of colour and gloss of the different coatings, it was used a spectrophotometer Uv-Vis-Nir Recording Spectrophotometer, UV-3100 by Shimadzu. The percentage of reflected light is collected at different wavelength (from 825 to 200 nm, with steps of 0,2 nm). It was examined three samples for each type of paint (Paint<sub>200%</sub>, CNT<sub>0,2%</sub>, Fe<sub>3</sub>O<sub>4</sub> 0,2%, Fe<sub>3</sub>O<sub>4</sub> 0,5).

In Figure 3.22 it is presented the variation of the reflection percentage with the wavelength graphs of the studied samples. The values entered here are the averages of the results obtained for each type of paint. Approaching the wavelengths of infrared (towards 700 nm) it can be seen, that above 660 nm, the nanopaint Fe<sub>3</sub>O<sub>4</sub> 0,2% reflects more light than the base paint Paint<sub>200%</sub>, while the other nanopaints have lower values than that for the Paint<sub>200%</sub>.

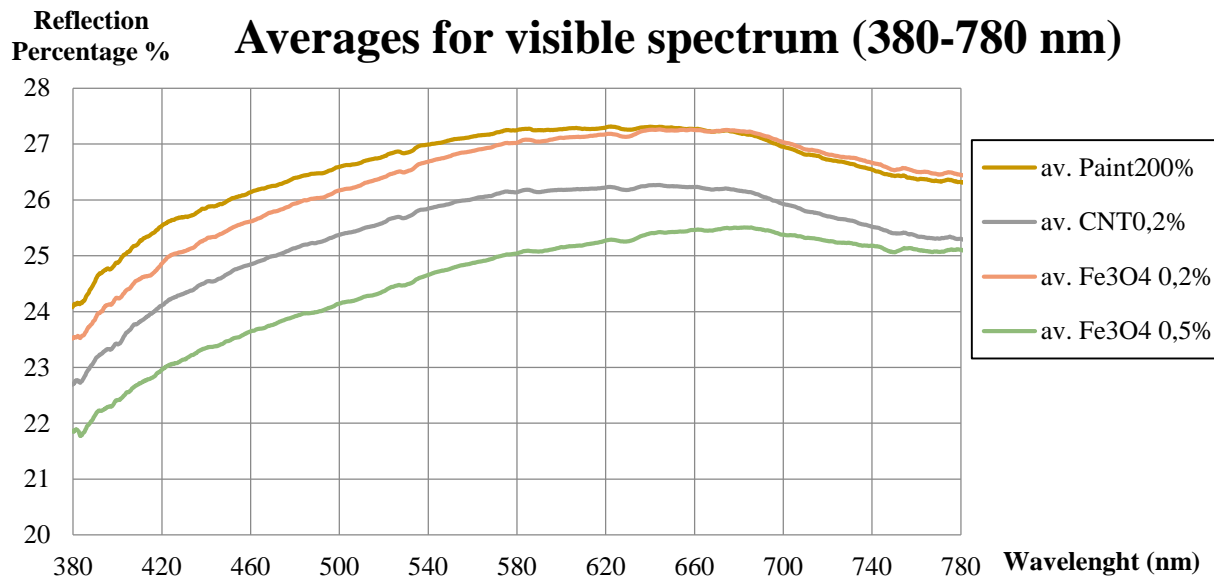


Figure 3.22 Light reflection in visible spectrum for Paint<sub>200%</sub>, CNT<sub>0,2%</sub>, Fe<sub>3</sub>O<sub>4</sub> 0,2% and Fe<sub>3</sub>O<sub>4</sub> 0,5%.

The base paint is the one that possesses better reflectivity values for almost the entire visible spectrum, a result that has already been anticipated in the previous analysis without the aid of instrumentation. In fact, with the naked eye it was clearly visible that Paint<sub>200%</sub> had a more gleaming and shiny surface than nanopaints.

### 3.4.3 Colour identification

It was possible to identify the colour of each paint using the values obtained from the measurement of the percentage of the reflected light. The data of the reflection and the wavelength of light (from 200 nm to 825 nm) were placed in a Matlab program that gave the values XYZ, Lab and RGB for each measurement of reflection of light. XYZ, Lab and RGB represent the colour spaces defined mathematically by the *Commission Internationale de l'Éclairage* (CIE) and the values corresponding to each letter are colour components that, combined together, describe the colour using an abstract mathematical model. Obtained the colour coordinates, it was possible to place them in an online software [42] that receives the XYZ values, Lab or RGB and releases the colour image defined by the mathematical coordinates. For the XYZ, "X", "Y" and "Z" represent the three primary colours (oversaturated colours) chosen by the CIE to generate all visible colours. For the Lab, "L" is the colour brightness from 0 (minimum brightness - black) to 100 (maximum-brightness white), "a" expresses the red colour when it is positive (up to  $+\infty$ ) and the green colour when it is negative (up to

$-\infty$ ) and "b" expresses the yellow colour when it is positive (up to  $+\infty$ ), and the blue colour when it is negative (up to  $-\infty$ ). "a" and "b" are chromaticity coordinates. RGB is a model to express the colours as percentage of red light (R), green light (G) and blue light (B). Its values range from 0 to 255 and can only be whole number values.

Using the program previously described, the colour coordinates were obtained, as averages of the colour coordinates of each individual sample. The RGB values of these coordinates have been rounded to the nearest whole number as the RGB.

It can be noted in Table 3.5 that the coordinates of the averages of the same type of paint, obtained by various processes, are equal to each other or similar, except for the coordinates of  $\text{Fe}_3\text{O}_4 0.2\%$ .

Table 3.5 Colour coordinates XYZ, Lab and RGB.

Paint	X	Y	Z	L	a	b	R	G	B
av.Paint <sub>200%</sub>	25,560	26,966	27,902	58,943	-0,030	1,558	143,000	142,000	138,000
Paint <sub>200%</sub>	25,560	26,966	27,902	58,943	-0,030	1,558	143,000	142,000	138,000
av.CNT <sub>0,2%</sub>	24,478	25,821	26,496	57,867	-0,015	1,885	141,000	140,000	135,000
CNT <sub>0,2%</sub>	24,478	25,821	26,496	57,867	-0,015	1,885	141,000	139,000	135,000
av.Fe <sub>3</sub> O <sub>4 0,2%</sub>	23,256	24,468	24,987	56,553	0,258	2,048	138,000	136,000	132,000
Fe <sub>3</sub> O <sub>4 0,2%</sub>	25,271	26,633	27,276	58,632	0,087	1,984	143,000	142,000	137,000
av.Fe <sub>3</sub> O <sub>4 0,5%</sub>	23,460	24,685	25,210	56,767	0,249	2,050	139,000	136,000	132,000
Fe <sub>3</sub> O <sub>4 0,5%</sub>	23,664	24,902	25,434	56,980	0,240	2,053	139,000	137,000	133,000

Analysing the standard deviation (SD) for the average coordinates of  $\text{Fe}_3\text{O}_4 0.2\%$ , it can be noted (Table 3.6) as the averages of the coordinates of the individual samples are more reliable than the coordinate values calculated on the averages of the percentage of light reflection. In fact, the SD  $\text{Fe}_3\text{O}_4 0.2\%$  values are lower than those of SD av.  $\text{Fe}_3\text{O}_4 0.2\%$  by at least one order of magnitude, therefore, only the values of  $\text{Fe}_3\text{O}_4 0.2\%$  (not av.  $\text{Fe}_3\text{O}_4 0.2\%$ ) were considered.

Table 3.6 Standard deviation of XYZ, Lab and RGB coordinates of  $\text{Fe}_3\text{O}_4 0.2\%$  and av. $\text{Fe}_3\text{O}_4 0.2\%$ .

	X	Y	Z	L	a	b	R	G	B
SD av. $\text{Fe}_3\text{O}_4 0.2\%$	2,027	2,177	2,302	2,090	0,171	0,064	5,354	5,686	5,066
SD $\text{Fe}_3\text{O}_4 0.2\%$	0,216	0,228	0,237	0,213	0,001	0,003	0,471	0,471	0,816

From table values, colour differences are notable compared to Paint<sub>200%</sub>, especially the brightness decreases ("L" values) with small percentages of nanoparticles. So it cannot be used CNTs and nano- $\text{Fe}_3\text{O}_4$  to produce nanocoatings with chrome effect, but should be used nanoparticles that affect less the colour of the paint.

### 3.4.4 Thickness

To measure the thermal conductivity of the paint, it was necessary to know the thickness of the paint layer. The thicknesses were determined with a help of an optical microscope (Nikon – Eclipse LV150) with an objective lens, Nikon – LU Plan Fluor 20X/0.45 A  $\infty/0$  BD. In Figure 3.23 it can be seen how it was determined the thickness of the nanopaints in different place of the layer.

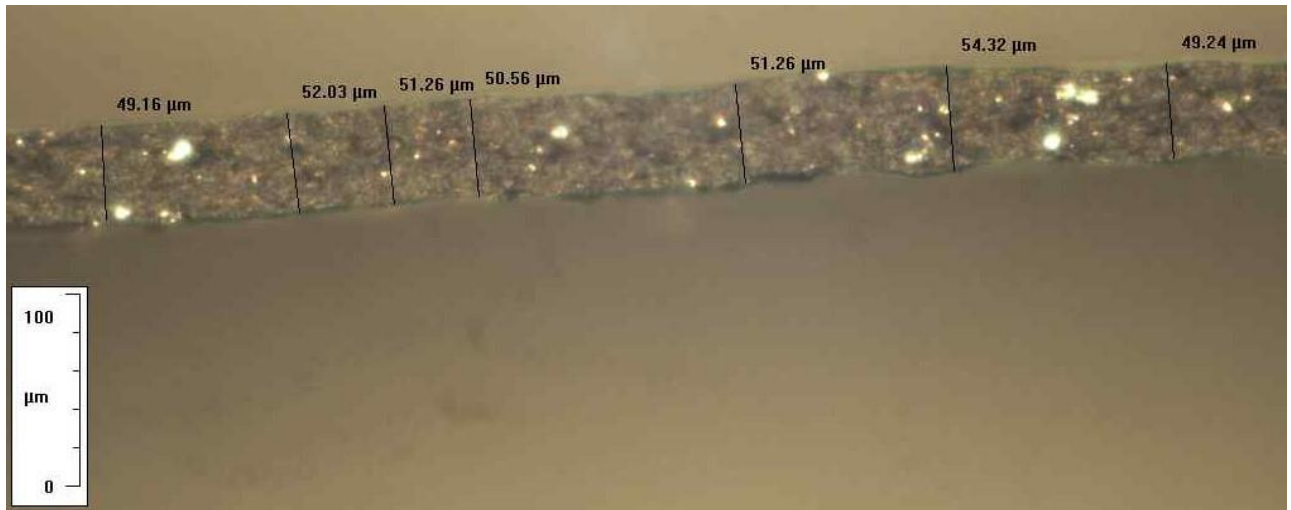


**Figure 3.23** Thickness measurement with the optical microscope “Nikon – Eclipse LV150” and the software “Perfect-Image V7.5”.

For each type of paint, four samples with a size of  $5 \times 3 \text{ mm}^2$  (approximately) were prepared and 25 measurements were made for each sample. With this procedure it was possible to derive the mean and standard deviation of the layer thickness.

It was analysed the samples: Paint<sub>200%</sub>, CNT<sub>0,2%</sub> and CNT<sub>1,0%</sub>. Table 3.7 summarizes the calculated thicknesses of the different samples.

**Table 3.7** Mean and the standard deviation of Paint<sub>200%</sub>, CNT<sub>0,2%</sub> and CNT<sub>1,0%</sub>.

Paint	$\Delta x_{av}$ [μm]	SD $\Delta x_{av}$ [μm]
Paint <sub>200%</sub>	41,19	3,99
CNT <sub>0,2%</sub>	76,71	11,59
CNT <sub>1,0%</sub>	88,56	8,62

The defect of these measurements is the inability to measure the thickness in the center of the specimens without breaking them. In fact, the thicknesses at the sides of the specimens were measured and from the values obtained were calculated the average  $\Delta x_{av}$  and the standard deviation SD  $\Delta x_{av}$ .

To get the averages calculated with values obtained all over the specimen, it was used a micrometer with resolution  $\pm 5 \mu\text{m}$  (Micrometer Mitutoyo). Averages ( $\Delta x_{av}$ ), standard deviations ( $SD \Delta x_{av}$ ) and uncertainties ( $U(\Delta x_{av})$ ) were measured for Paint<sub>200%</sub>, CNT<sub>0,1%</sub>, CNT<sub>0,2%</sub>, CNT<sub>0,3%</sub>, CNT<sub>0,4%</sub>, CNT<sub>0,5%</sub>, CNT<sub>0,7%</sub> and CNT<sub>1,0%</sub>, summarized in Table 3.8.

**Table 3.8** Averages, standard deviations and uncertainties for paints and nanopaints.

Paint	$\Delta x_{av} [\mu\text{m}]$	$SD \Delta x_{av} [\mu\text{m}]$	$U(\Delta x_{av}) [\mu\text{m}]$
Paint <sub>200%</sub>	43,97	2,36	10,03
CNT <sub>0,1%</sub>	79,16	7,53	10,14
CNT <sub>0,2%</sub>	88,86	6,87	10,13
CNT <sub>0,3%</sub>	87,7	6,19	10,11
CNT <sub>0,4%</sub>	94,45	6,24	10,13
CNT <sub>0,5%</sub>	88,58	6,37	10,1
CNT <sub>0,7%</sub>	113,26	10,05	10,23
CNT <sub>1,0%</sub>	115,93	9	10,22

Comparing the values of Paint<sub>200%</sub>, CNT<sub>0,2%</sub> and CNT<sub>1,0%</sub> of Table 3.7 and Table 3.8, high differences in values of average are noted above all for the thicknesses of the nanopaints.

### 3.4.5 Thermal conductivity of the solid paint ( $\lambda_s$ )

The thermal properties were performed using the Gustafsson Probe method (or Hot Disk) with the Thermal Constant Analyzer TPS 2500S. This method uses an electrically conducting pattern (Nickel) element acting both as a temperature sensor and heat source, insulated with two thin layers of Kapton ( $70 \mu\text{m}$ ). The samples, with the sensor in the middle, are then placed between the substrate halves (Figure 3.24).

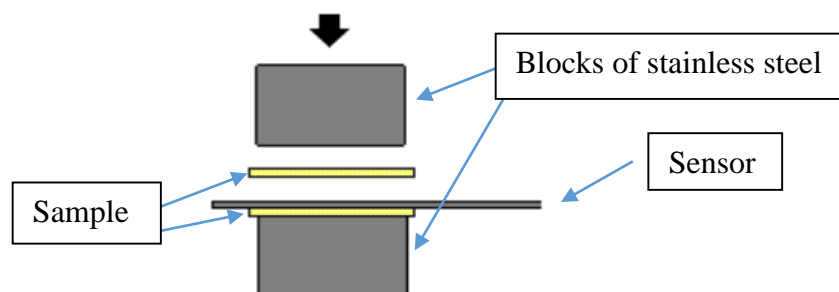


**Figure 3.24** Mounting the samples (yellow).

The thermal conductivity,  $\lambda_s$ , of thin samples (the paint was peeled from the substrate) can be extracted from the following formula:

$$\frac{P}{2} = A * \lambda_s * \frac{\Delta T}{\Delta x}$$

where P is the total power output, A is the area of the conducting pattern,  $\lambda_s$  is the thermal conductivity of the thin sample,  $\Delta T$  is the fully developed temperature difference across one of the insulating layers and  $\Delta x$  is the thickness of the thin sample pieces. The minimum thickness layer 25  $\mu\text{m}$ , with a resolution of  $\pm 0,5 \mu\text{m}$ .

The measurements were performed for the paints: Paint<sub>200%</sub>, CNT<sub>0,1%</sub>, CNT<sub>0,2%</sub>, CNT<sub>0,3%</sub>, CNT<sub>0,4%</sub>, CNT<sub>0,5%</sub>, CNT<sub>0,7%</sub> and CNT<sub>1,0%</sub>. In Table 3.9 are shown the main results of the thermal conductivity of these samples, with uncertainty U( $\lambda_s$ ), calculated taking into account the uncertainty of the thickness measured with the micrometer and it's shown the percentage variation of  $\lambda_s$  related to  $\lambda_s$  of Paint<sub>200%</sub>.

**Table 3.9** Thermal conductivity, uncertainty and percentage enhancement of  $\lambda_s$ .

Paint	$\lambda_s$ [W/mK]	U( $\lambda_s$ ) [W/mK]	$\lambda_s$ Enhancement %
Paint <sub>200%</sub>	0,092	0,021	0
CNT <sub>0,1%</sub>	0,154	0,02	+67,39
CNT <sub>0,2%</sub>	0,123	0,014	+33,7
CNT <sub>0,3%</sub>	0,145	0,017	+57,60
CNT <sub>0,4%</sub>	0,162	0,017	+76,09
CNT <sub>0,5%</sub>	0,151	0,017	+64,13
CNT <sub>0,7%</sub>	0,192	0,017	+108,7
CNT <sub>1,0%</sub>	0,101	0,009	+9,78

As it can be seen from the results, with the addition of the nanoparticle, the thermal conductivity increases till the 0,7% weight concentration and then decreases. In Figure 3.25 you can see the values of  $\lambda_s$  for the corresponding mass percentages of CNTs, where there is a percentage around 0,7 wt% to which corresponds the maximum increase of thermal conductivity. It is possible to fit these values with polynomial curves with different order, but it's necessary to know the exact values of percolation

threshold and of the maximum enhancement and even more values with different wt% are needed to have a complete trendline to justify the choice of the polynomial's order.

It is worth to mention also that as the paint is applied to the substrate (polymeric peace), the diluent evaporates, and for that reason, the weight percentage of the nanoparticles into the nanopaints will increases considerably. Indeed, it can be said that with high values of weight percentages, the nanopaint changed its thermal properties.

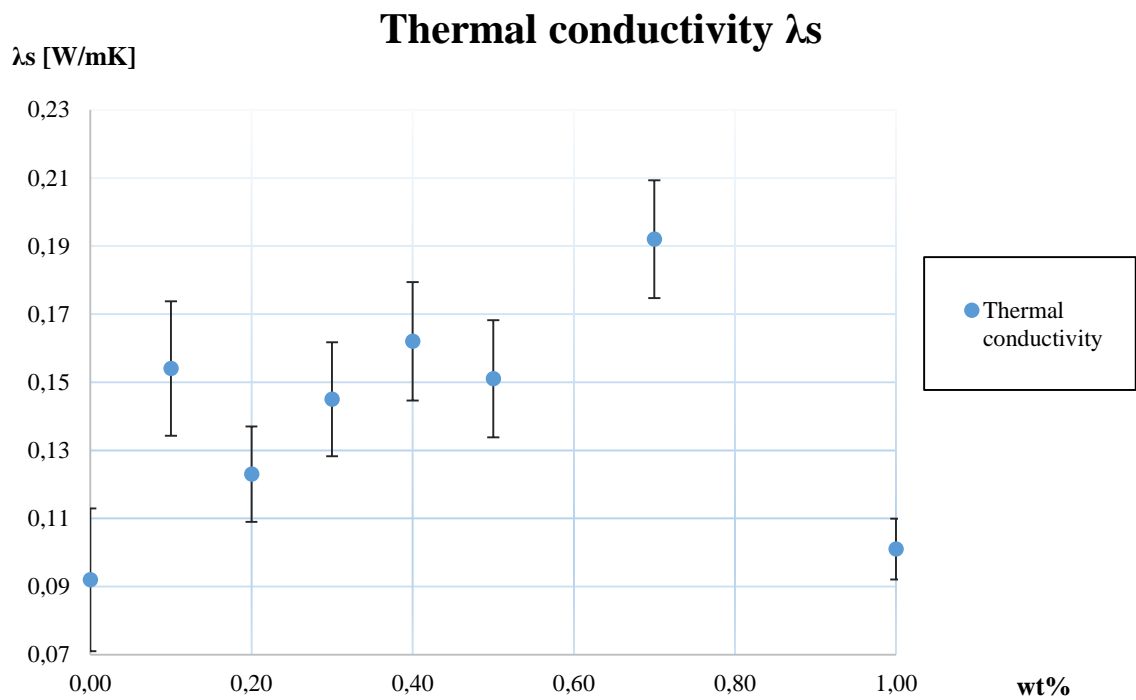


**Figure 3.25** Values of thermal conductivity varying the mass percentage of CNTs.

These specimens were produced by following the same procedures previously used for other tests, but with the difference that the number of paint applications has been doubled to four steps, in order to obtain a thickness greater than the limit for  $\lambda_s$  measurement.

The worsening of thermal conductivity by adding the CNTs (over 0,7wt%) should be justified by the increase of contact resistance resulting from the weak bonds between the CNTs. [43]

### 3.4.6 Thermal conductivity of the liquid paint ( $\lambda_l$ )

It was considered useful to measure the thermal conductivity also in the liquid phase, to have an index of possible increments of thermal conductivity of the nanopaint solid phase. To do this, it was used the thermal analyzer KD2 Pro, that applied the transient wire method to measure the thermal conductivity.

The instrument collects data every 15 minutes and at least 5 measurements of thermal conductivity of each sample were collected. The results are summarized on Table 3.10.

**Table 3.10** Thermal conductivity of paints and nanopaints in liquid phase with measurement's temperature and percentage variation related to Paint<sub>200%</sub>.

Paint	$\lambda_l$ [W/mK]	U( $\lambda_l$ ) [W/mK]	T [°C]	$\lambda_l$ Enhancement%
<b>Paint<sub>0%</sub></b>	0,154	±0,001	18,7	6,21
<b>Paint<sub>200%</sub></b>	0,145	±0,001	18,5	0
<b>CNT<sub>0,1%</sub></b>	0,15	±0,001	19,8	3,45
<b>CNT<sub>0,2%</sub></b>	0,151	±0,001	19,3	4,14
<b>CNT<sub>0,3%</sub></b>	0,152	±0,001	19,6	4,83
<b>CNT<sub>0,4%</sub></b>	0,155	±0,001	19,8	6,9
<b>CNT<sub>0,5%</sub></b>	0,157	±0,001	19,8	8,28
<b>CNT<sub>0,7%</sub></b>	0,161	±0,001	18,7	11,3
<b>CNT<sub>1,0%</sub></b>	0,166	±0,001	20,3	14,48
<b>Fe<sub>3</sub>O<sub>4</sub> 0,2%</b>	0,146	±0,001	18,5	0,69
<b>Fe<sub>3</sub>O<sub>4</sub> 1,0%</b>	0,147	±0,001	18,5	1,38

As it can be observed from the data in Table 3.10, the addition of diluent to the base coat (Paint<sub>0%</sub>) caused a decrease of  $\lambda_l$ , a reduction which is significant as it corresponds to 6,21%. It is useful to compare the paint containing nanoparticles with Paint<sub>200%</sub>, since the diluent is essential for the application of paints.

The results show that the addition of CNTs clearly increase the thermal conductivity of the base paint. However, the addition of the Fe<sub>3</sub>O<sub>4</sub> nanoparticles does not change significantly the thermal conductivity of the nanopaint.

In Figure 3.26 there is a graph that shows the thermal conductivity of paint and nanopaint in the liquid phase, with the respective error bars. For nanopaint with CNTs has been inserted a linear trend line (LinearCNTs) to obtain an assessment of the development of the thermal conductivity  $\lambda_l$ . As it can be seen, the values obtained for  $\lambda_l$  do not vary much from the trendline.

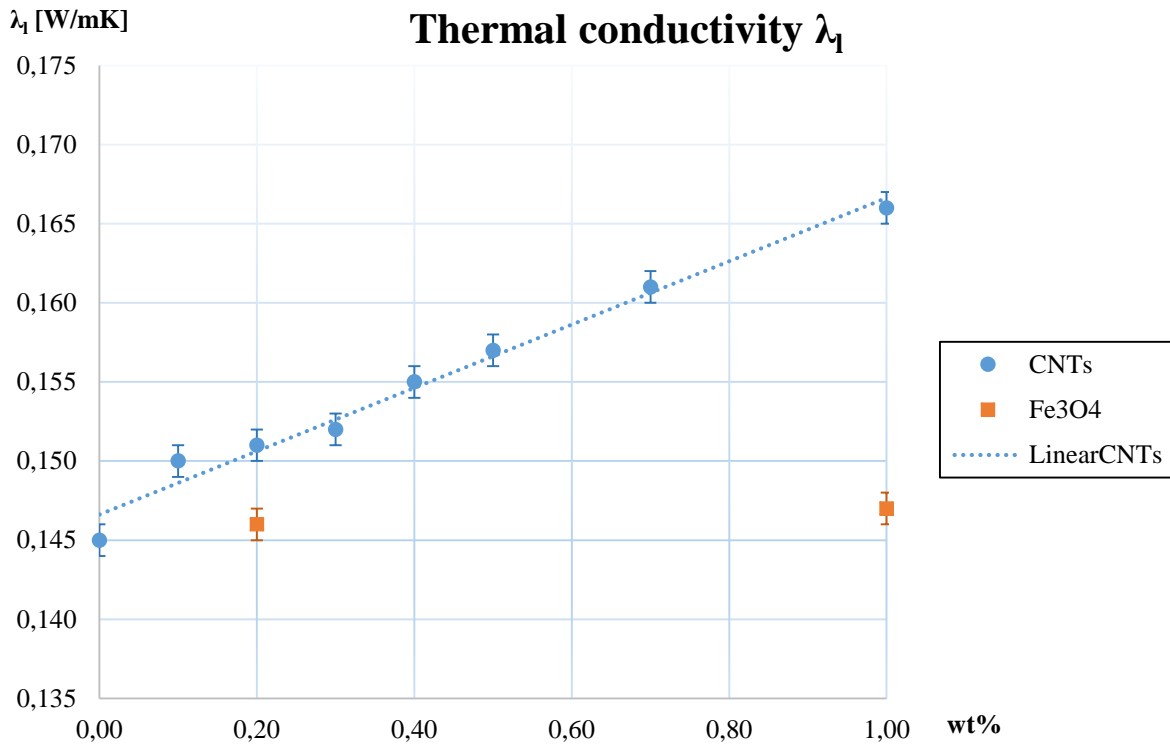


**Figure 3.26** Thermal conductivity for paints and nanopaints in liquid phase.

### 3.4.7 Electrical conductivity measurements

The DC electrical conductivity ( $\sigma_{dc}$ ) of the samples was measured with a Keithley 6517B electrometer, in the temperature range between 170 and 380 K, using a nitrogen bath cryostat setup. During the measurements, the samples were kept in a helium atmosphere to minimize thermal gradients. The  $\sigma_{dc}$  can be calculated, as well as the density.

$$\sigma_{dc} = \frac{I}{V} * \frac{d}{A} = \frac{1}{\rho_{dc}}$$

$$\rho_{dc} = \frac{A}{d} * R$$

$V$  is the electric potential difference,  $I$  is the current intensity,  $d$  is the distance of the points among which the voltage is measured,  $A$  is the area of the section of the sample perpendicular to the direction of the current,  $\rho_{dc}$  is the electrical resistivity (direct current) and  $R$  is the electric resistance. The AC electrical conductivity ( $\sigma_{ac}$ ) and impedance measurements were also performed in the temperature

range of 170 to 380 K, using the same bath cryostat, with a Network Analyzer, Agilent 4294, operating between 100 Hz and 1 MHz in the  $C_p$ - $R_p$  configuration (capacitance in parallel with resistance). In both measurements the temperature of the samples was controlled by an Oxford Research IT-C4.

The real and complex parts of the permittivity were calculated using the following relations:

$$\epsilon' = \frac{d}{S} * \frac{C_p}{\epsilon_0}$$

$$\epsilon'' = \frac{d}{S} * \frac{1}{\omega R_p \epsilon_0}$$

with  $C_p$  the measured capacitance,  $R_p$  the resistance,  $d$  the sample thickness,  $S$  the electrode area,  $\omega$  the frequency and  $\epsilon_0$  the vacuum permittivity ( $8.8542 \times 10^{-12}$  F/m).

The AC conductivity,  $\sigma_{ac}$ , was calculated using the relation:

$$\sigma_{ac} = \epsilon'' \omega \epsilon_0$$

In Figure 3.27 it is shown the graph of the dc conductivity with temperature, for the base paint, at different voltages. As it can be observed, the DC conductivity decreases from 170 K until  $\sim 290$  K with the increase of the temperature, which is a typical behavior for metallic materials.

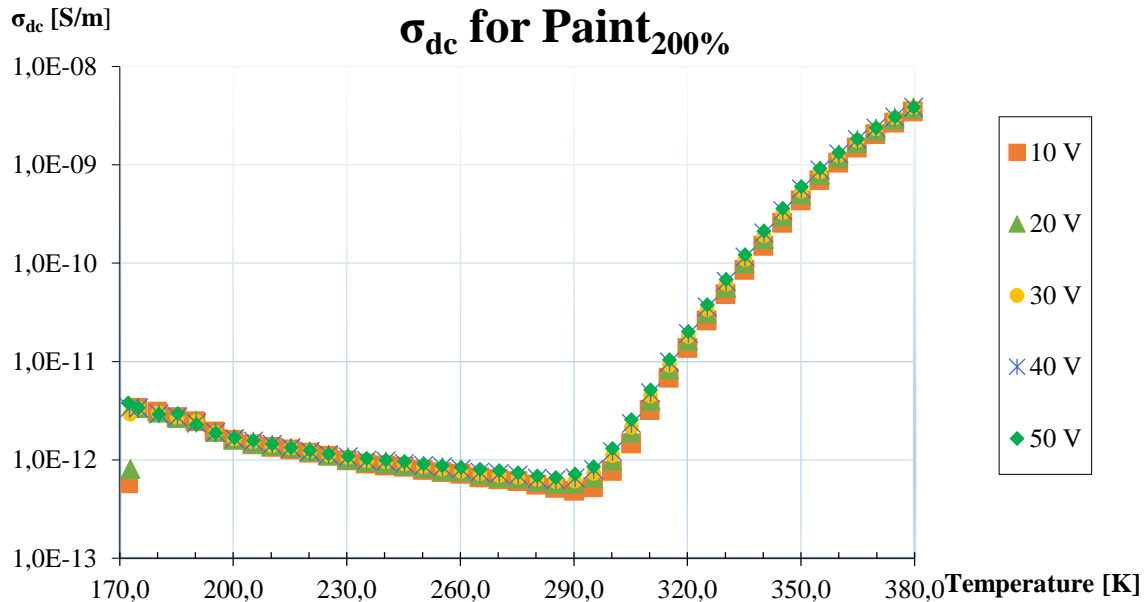


**Figure 3.27** Behaviour of  $\sigma_{dc}$  (Paint<sub>200%</sub>) changing the temperature between 170 K to 380 K. The measurements were done for 10 V, 20 V, 30 V, 40 V and 50 V.

The DC conductivity of the sample shows a sharply increase, which starts at  $\sim 300$  K. This indicates that at this temperature there is a structural change in the polymer. Moreover, above this temperature

there must be some charge carriers which become thermally activated and become the predominant conduction type.

In Figure 3.28 it is shown the relation between the current and the applied voltage, for the base paint, at room temperature. It can be seen that the sample follows an ohmic behavior, so Paint<sub>200%</sub> can be classified as an ohmic conductor: the potential difference at the terminals of a current-carrying conductor is directly proportional, according to the electric resistance of the conductor, to the intensity of the current.

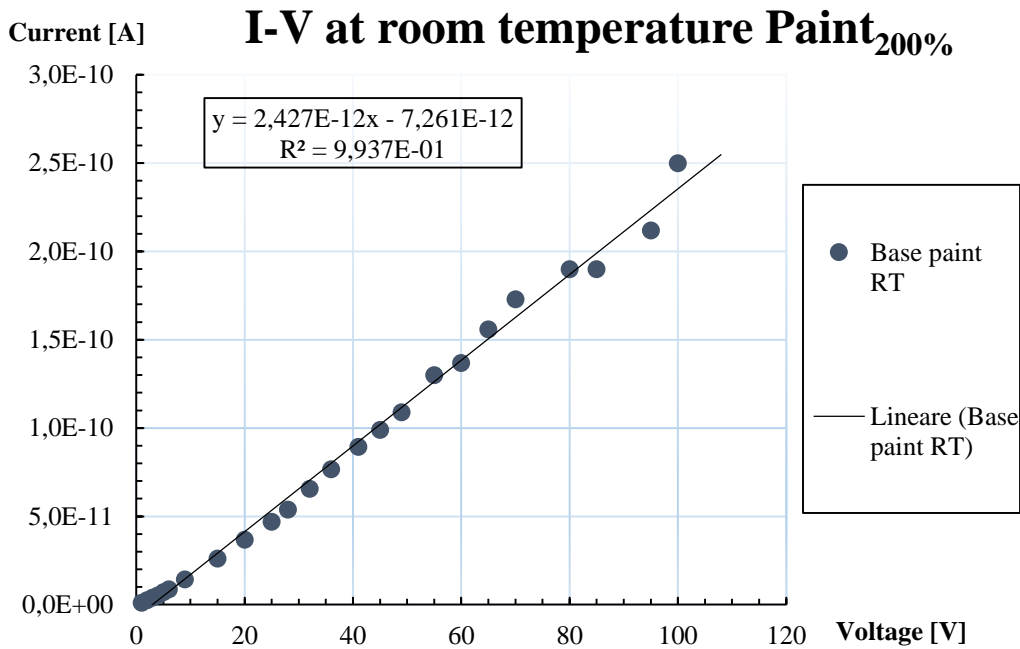
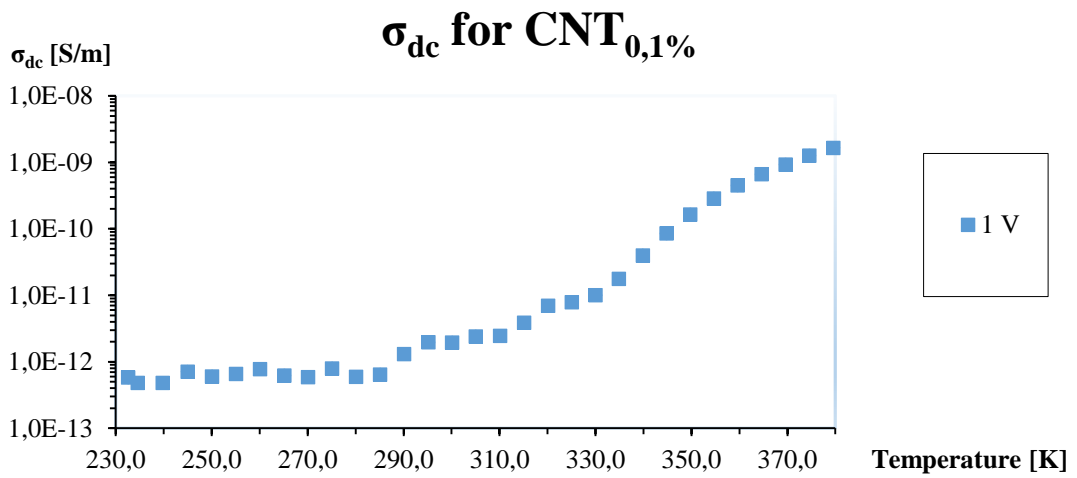
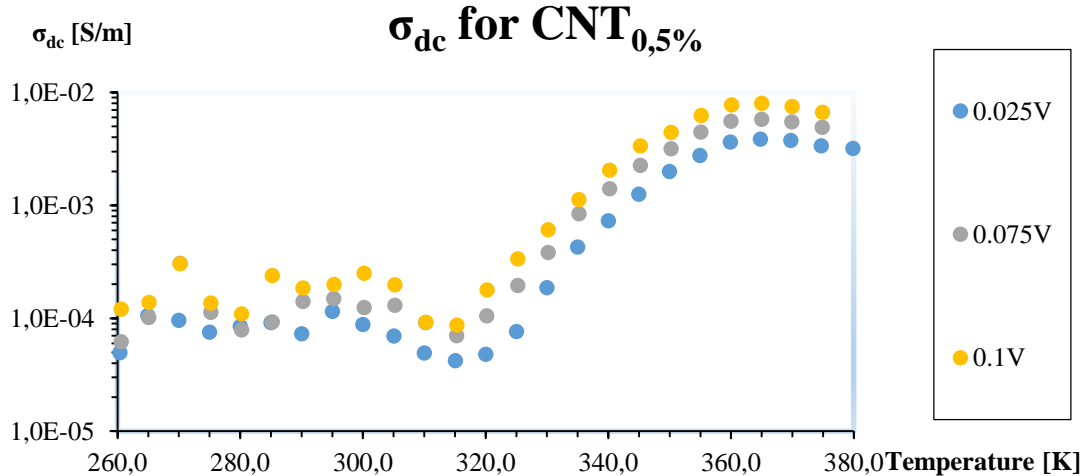


Figure 3.28 I-V correlation at room temperature for Paint<sub>200%</sub>.

The direct current electrical conductivity analysis was also carried out for CNT<sub>0,1%</sub>, CNT<sub>0,5%</sub> and CNT<sub>1,0%</sub>, with the corresponding results in Figure 3.29, Figure 3.30 and Figure 3.31. For CNT<sub>0,1%</sub> there is not a substantial increase of  $\sigma_{dc}$  compared to Paint<sub>200%</sub>, in fact, the values are within the same orders of magnitude and the raising of  $\sigma_{dc}$  due to temperatures is similar to that of Paint<sub>200%</sub>. This suggests that with this mass percentage of CNTs there is still not the effect of percolation that lifts  $\sigma_{dc}$ , while at higher percentages (0,5 wt% and 1,0 wt%) it can be seen from the change of 6/8 orders of magnitude of the results (Figure 3.30 and Figure 3.31).



**Figure 3.29** Behaviour of  $\sigma_{dc}$  (CNT<sub>0,1%</sub>) changing the temperature between 230 K to 380 K. The measurements were done for 1 V.



**Figure 3.30** Behaviour of  $\sigma_{dc}$  (CNT<sub>0,5%</sub>) changing the temperature between 260 K to 380 K. The measurements were done for 0,025 V, 0,075 V and 0,1 V.

The DC conductivity of the samples doped with 0,5 wt% and 1,0 wt% CNTs are significantly greater than that of the base paint. As shown in Figure 3.30 and Figure 3.31, from 170 to 305/315 K, the DC conductivity is around  $10^{-3}$ - $10^{-4}$  S/m, which represents an increase of ~8 order of magnitude when compared to the base sample.

At around 315 K, the conductivity of the doped paint with 0,5 wt% starts to increase, and at ~360 K the conductivity seems to saturate. At this given temperature, all available charge carriers are in conduction band. The same effect can be seen for the paint with 1,0 wt%, but at 305 K and ~355 K.

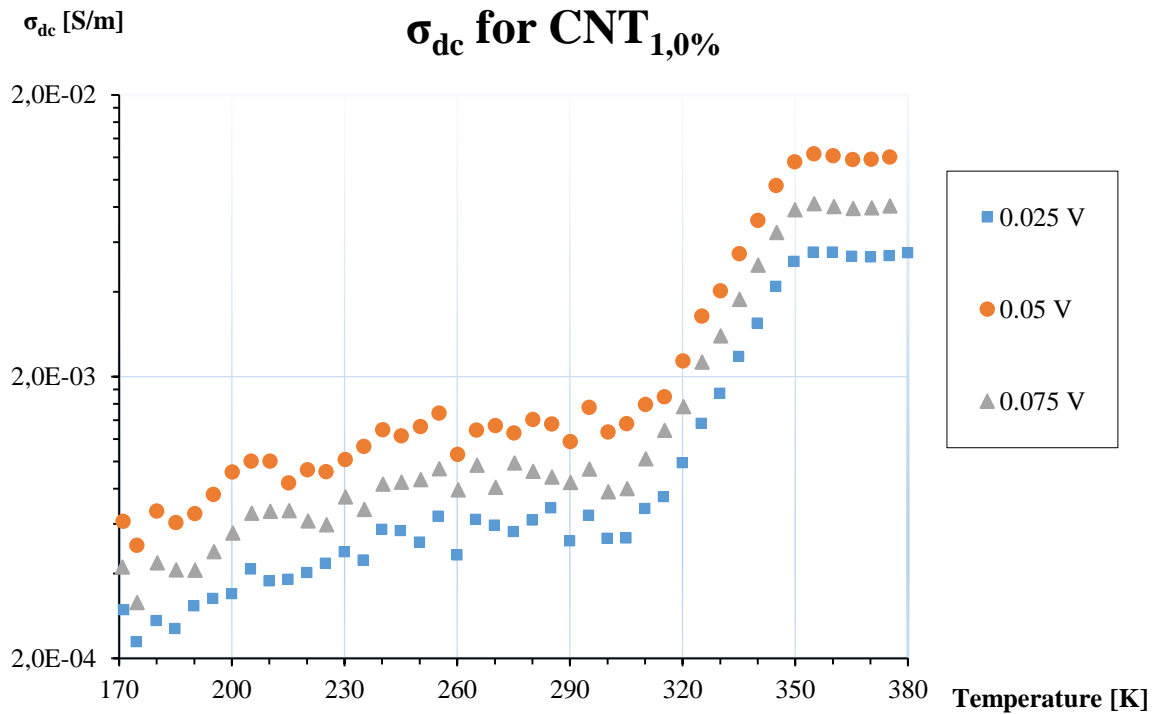


**Figure 3.31** Behaviour of  $\sigma_{dc}$  (CNT<sub>1,0%</sub>) changing the temperature between 170 K to 380 K. The measurements were done for 0,025 V, 0,05 V and 0,075 V.

The conductivity dependence of the applied electric field (voltage) is not linear, and the results showed the existence of a maximum around 0.05 V for CNT<sub>1,0%</sub>, which has a rise in the electric conductivity around 305 K, while around 350 K it saturates.

The raising of  $\sigma_{dc}$  related to temperature for both CNT<sub>0,5%</sub> and CNT<sub>1,0%</sub> may be due to the increase of percolation of CNTs, probably through the softening of the paint at 315 K for 0,5 wt% and at 305 K for 1,0 wt%. In fact, a softening of the paint, due to the glass transition temperature, allows the carbon nanotube to move and reorient itself in the matrix, up to reach the optimization of percolation around 355/360 K. When the maximum percolation is reached, the electric conductivity saturates, and it varies only varying the voltage.

The I-V correlation of the CNT<sub>1,0%</sub>, was performed also at room temperature. Two measurements were made, and their results were very similar as shown in Figure 3.32. As it can be seen this sample does not follow an ohmic behavior because the current is not directly proportional to the potential difference.

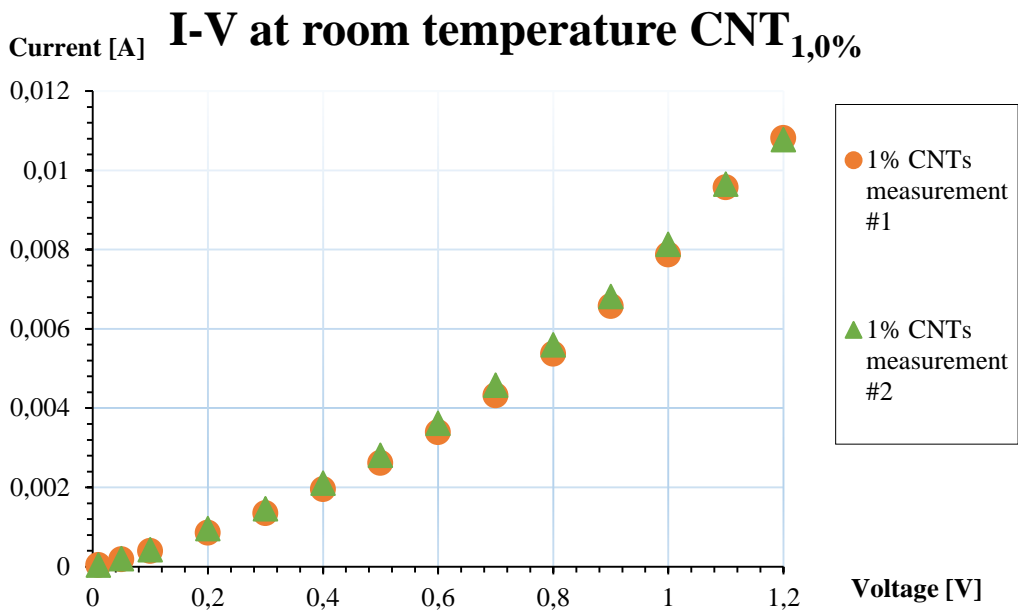


Figure 3.32 I-V correlation at room temperature for CNT<sub>1,0%</sub>.

The AC conductivity measurements show that, for CNT<sub>1,0%</sub>, there is a serious increase of the  $\sigma_{ac}$  values (~4 orders of magnitude), as shown in Figure 3.33.

### $\sigma_{ac}$ for Paint200% and CNT1,0%

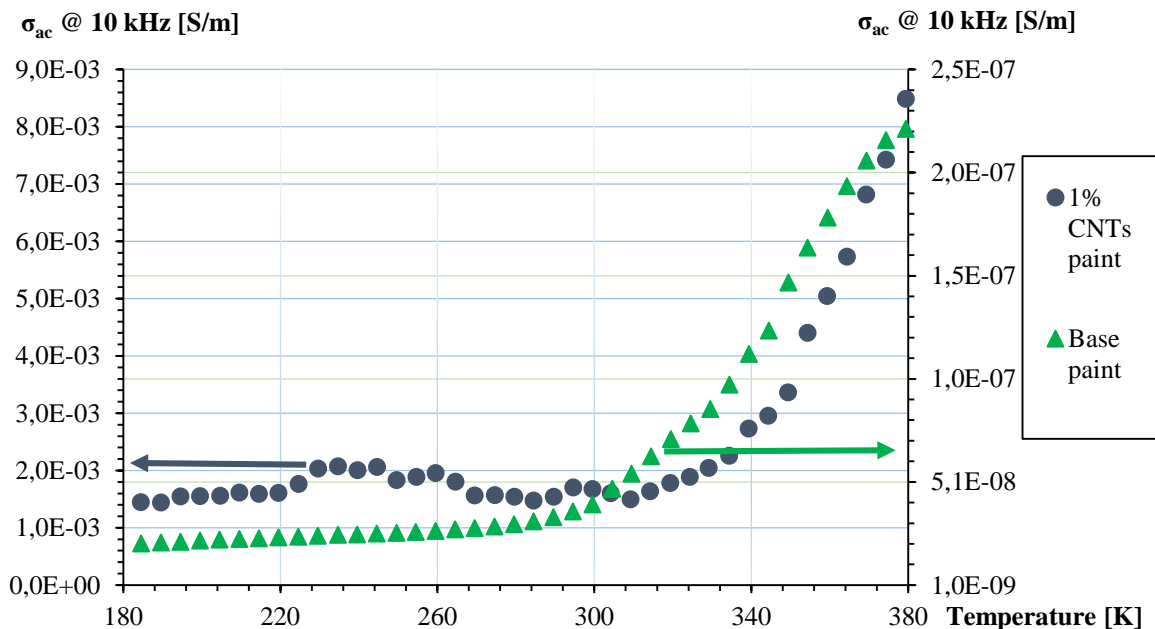
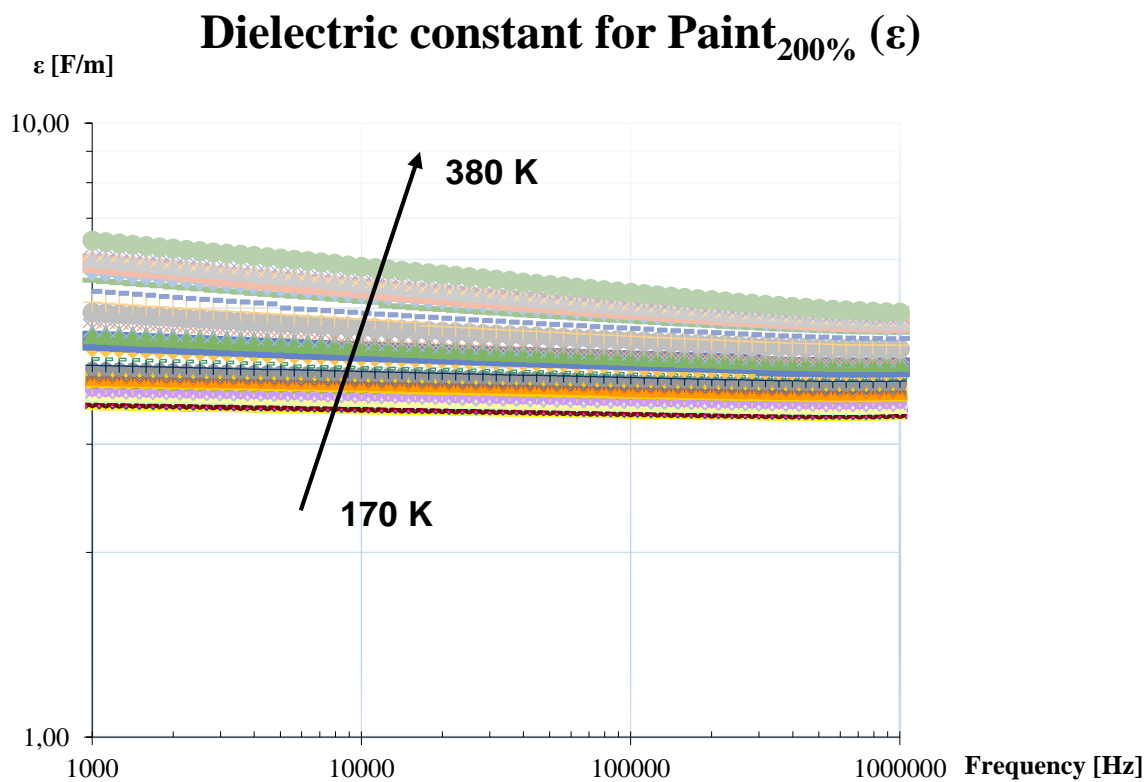


Figure 3.33 Behaviour of  $\sigma_{ac}$  (green triangles: Paint<sub>200%</sub>; blue circles: CNT<sub>1,0%</sub>) changing the temperature between 170 K to 380 K.

Similarly, to the DC case, for temperatures above 300 K there is a large increase of the electrical conductivity.

The dielectric constant of Paint<sub>200%</sub> decreases with the increase of the frequency, and increases with the increase of the temperature, showing that the temperature can activate a polarization mechanism.

For the base paint, the maximum dielectric constant was ~10, observed at 370 K and 1000 Hz (Figure 3.34). At the same measurement conditions, the 1% doped sample, presented a dielectric constant of ~150 (15x greater).



**Figure 3.34** Dielectric constant ( $\epsilon$ ) of Paint<sub>200%</sub> varying frequency from  $10^3$  Hz to  $10^6$  Hz, and varying temperature from 170 K to 380 K.

As shown in Figure 3.35, the sample with CNTs revealed a higher dispersion for frequencies lower than 1 kHz, which indicates the existence of a strong contribution from electrode polarization or interfacial polarization effects assigned to the presence of CNTs.

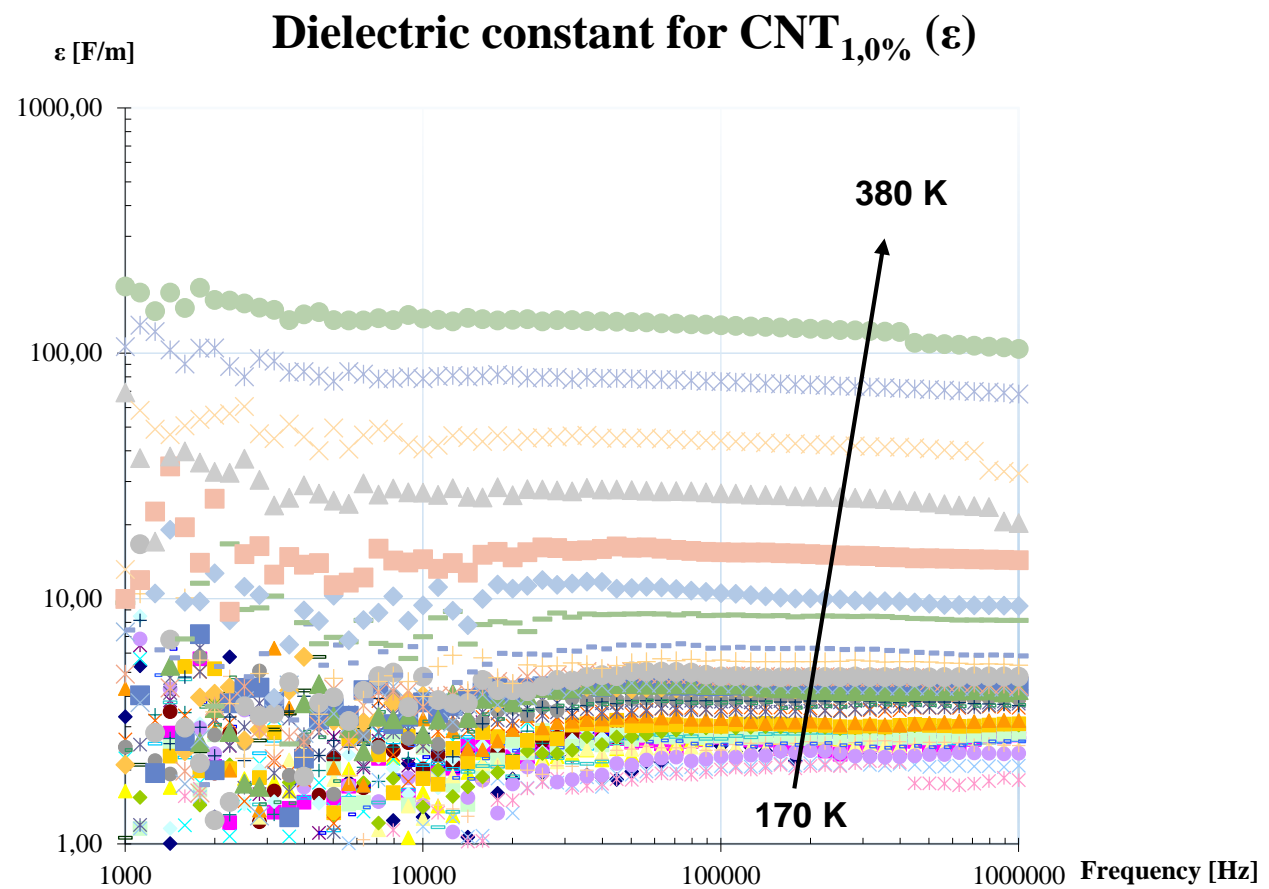


**Figure 3.35** Dielectric constant ( $\epsilon$ ) of CNT<sub>1,0%</sub> varying frequency from  $10^3$  Hz to  $10^6$  Hz, and varying temperature from 170 K to 380 K.

In Figure 3.36 and Figure 3.37 the dielectric constants of Paint<sub>200%</sub> and CNT<sub>1,0%</sub> are compared with changes in temperature for the fixed values of 10000 Hz and 100,000 Hz. It is noted that the dielectric constant increases with the temperature increasing and that as the frequency increases, the temperature, at which  $\epsilon$  of CNT<sub>1,0%</sub> exceeds  $\epsilon$  of Paint<sub>200%</sub>, decrease.

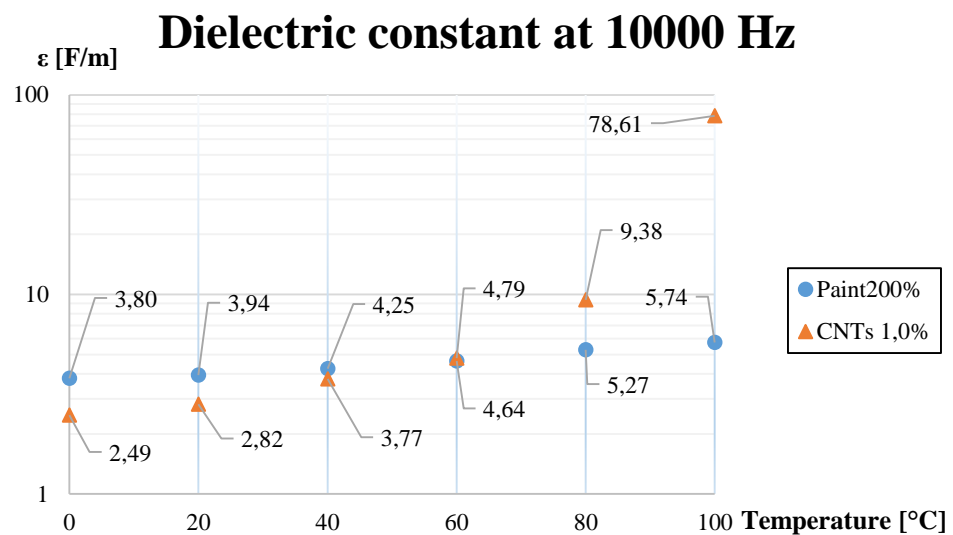


Figure 3.36 Dielectric constant at 10000 Hz

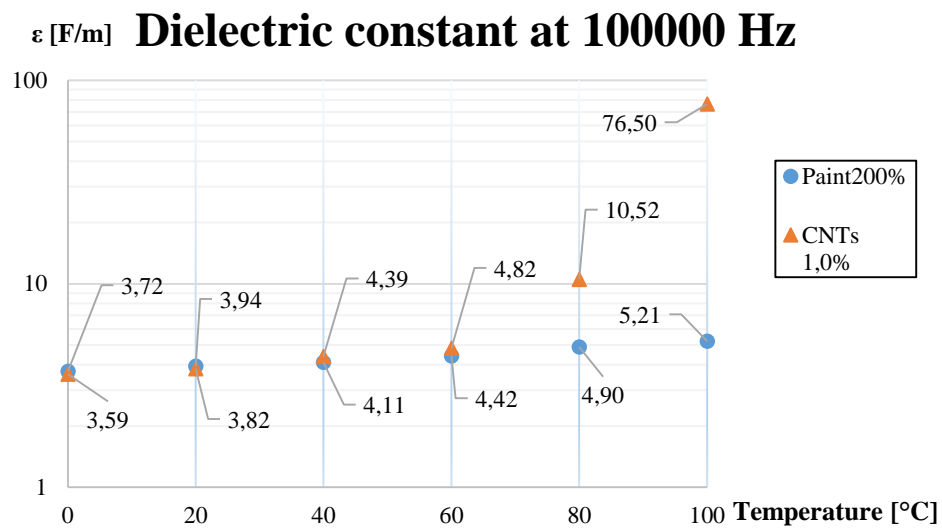


Figure 3.37 Dielectric constant at 100000 Hz

## 4 Discussion of the results

### 4.1 Nanopaint preparation

The mixing of the nanoparticles is the crucial part in the preparation of the nanopaint, in fact, different tools and different procedures were used to obtain a paint as homogeneous as possible. The first phase, which consists in mixing the base paint with the diluent, may be conducted with a magnetic stirrer for about 30 minutes. It was not necessary to produce coatings with different amounts of diluent as it evaporates during the application on the substrate and the percentage of diluent recommended by the manufacturer was used (Paint<sub>200%</sub>). For the mixing of the nanoparticles, initially an ultrasonic vibrator was used, but tended to overheat the paint with the risk of the diluent to evaporate, then a water bath was used together with ultrasonic vibrator to prevent overheating. Also incorporating the magnetic stirrer, it was possible to facilitate the mixing and dispersion of the nanoparticles, but it was not possible to use it with ferromagnetic particles as Fe<sub>3</sub>O<sub>4</sub>, since the magnetic field generated by the instrument would have limited or prevented proper mixing. As an alternative, an ultrasonic-bath was used, that mixed the nanoparticles using ultrasound without causing overheating of the paint. Furthermore, to improve such dispersion process, during the ultrasonic bath, it was possible to manually mix the paint with a glass stick (it was not possible to perform the same process with ultrasound vibrator). Therefore, in the preparation of nanopaint, it was followed the procedure which included the use of ultrasonic-bath with manual mixing for 30 minutes of mixing.

### 4.2 Colour analysis

In addition to the analysis of the thermal conductivity, it is necessary to take into account the change of paint colour when nanoparticles are added. The use of these paints has the purpose to protect the substrate, but the aesthetic factor is not less important. In fact, the chrome plating is considered as a process that gives prestige to chromed object, pushing up the price of the finished product. For this reason, the colour changes must be limited as much as possible. Firstly specimens coated with two different types of paint were prepared, as seen in Figure 4.1, Figure 4.2 and Figure 4.3. In all three figures, in the left part of the specimens, the Paint<sub>200%</sub> paint has been applied, while in the right side, paints loaded with nanoparticles have been applied.

With a first comparison it can be seen that paints containing only 0,2% of CNTs and 0,2% of Fe<sub>3</sub>O<sub>4</sub> are darker and less bright than Paint<sub>200%</sub>.

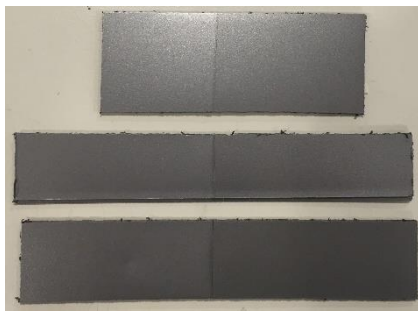


**Figure 4.1** Comparison of Paint<sub>200%</sub> - Fe<sub>3</sub>O<sub>4</sub> 0,2%.

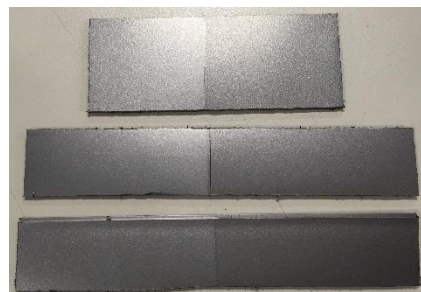


**Figure 4.2** Comparison of Paint<sub>200%</sub> - Fe<sub>3</sub>O<sub>4</sub> 0,5%.



**Figure 4.3** Comparison of Paint<sub>200%</sub> - CNT<sub>0,2%</sub>.

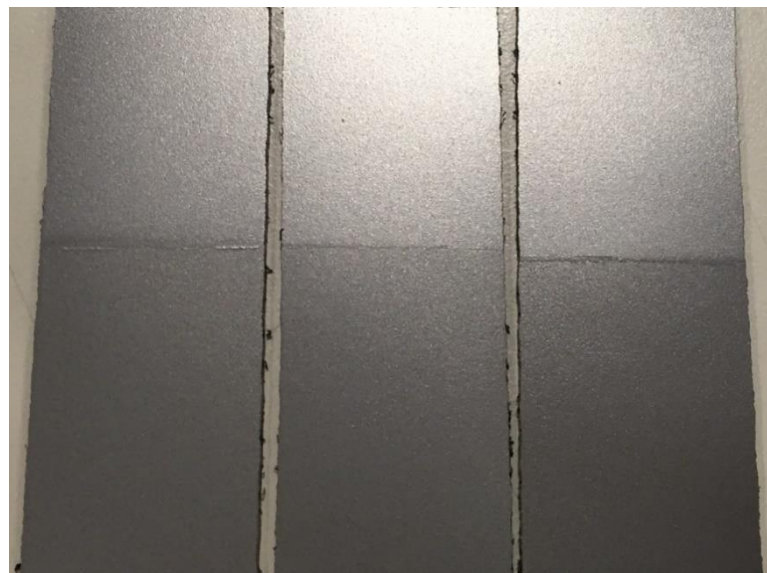


**Figure 4.4** Comparison of Paint<sub>200%</sub> and nanopaint. Left: Paint<sub>200%</sub> - CNT<sub>0,2%</sub>. Centre: Paint<sub>200%</sub> - Fe<sub>3</sub>O<sub>4</sub> 0,2%. Right: Paint<sub>200%</sub> - Fe<sub>3</sub>O<sub>4</sub> 0,5%.

It is still more evident how the colour changes with the addition of different nanoparticles with different dosages. In Figure 4.4, the upper part of the samples consists of Paint<sub>200%</sub>, the lower part by nanopaint. The specimen on the right presents the duller nanopaint, it is loaded with 0,5 wt% of Fe<sub>3</sub>O<sub>4</sub>. The colour change is a consequence not acceptable for a paint that is intended for aesthetic use. It is necessary in the future to analyse paint containing nano-powders presenting colours as similar as to grey chrome paint to avoid or at least limit such an evident discolouration.

In the analysis of light reflection, it was found a decrease in reflectivity of the paint when just 0,2 wt% of ENPs were added and the resulting change of colour was confirmed by RGB/Lab/XYZ analysis. Considering the brightness L of the Lab coordinates, all nanopaint have values of L less than Paint<sub>200%</sub>, index that the brightness is reduced because the addition of ENPs. Only Fe<sub>3</sub>O<sub>4</sub> 0,2% values

are obtained almost equal to those of Paint<sub>200%</sub>, but by increasing the dose to 0,5 wt% (Fe<sub>3</sub>O<sub>4</sub> 0,5%) the coordinates of the colour change dramatically. This highlights how nanoparticles used in this work are not suited to the required applications, since they generate substantial colour changes already with minimum percentages of colour. For this reason, in this work we have focused on the production and analysis process of the nanopaint, a process that can be used for future work with different nanoparticles that do not alter the colour in limited doses (as example nano-Al).

### 4.3 Thermal conductivity

As has been noted in the analysis of the results, the thermal conductivity of the paints had the same order of magnitude when it was measured in liquid or solid phase. However, the comparison should be conducted valuating the changes of wt% of nanoparticles after the diluent evaporation. In fact, after drying, the paint in the solid phase is no longer composed of two parts of diluent and a part of pure paint, but only pure paint, since the diluent is evaporated to allow solidification. The removal of the diluent is a very decisive factor on the preparation of nanopaint, as the percentage mass (or volume) of the nanoparticles changes from the initial values. In fact, the nanopaint initially with the 1,0 wt% of CNTs, after solidification, reaches ~3 wt%.

In Figure 4.5 there is the comparison between  $\lambda_s$  and  $\lambda_l$  of the nanopaint with the CNTs, in which the weight percentages of the solid phase were multiplied per 3 in order to have the approximation of the weight percentage after the diluent evaporation. As it can be seen, the values of solid and liquid phase don't match each other, but the trend of both show an enhancement of thermal conductivity when the CNTs' weight percentage increase. For  $\lambda_l$  values it is not possible to evaluate a maximum with those wt%, while in solid phase it is possible to estimate a maximum around 0,7 wt%, in fact to that weight percentage corresponds an enhancement of 108,7% respectively to the  $\lambda_s$  of Paint<sub>200%</sub>.

## $\lambda$ [W/mK] Comparison of $\lambda_s$ and $\lambda_l$ for CNTs

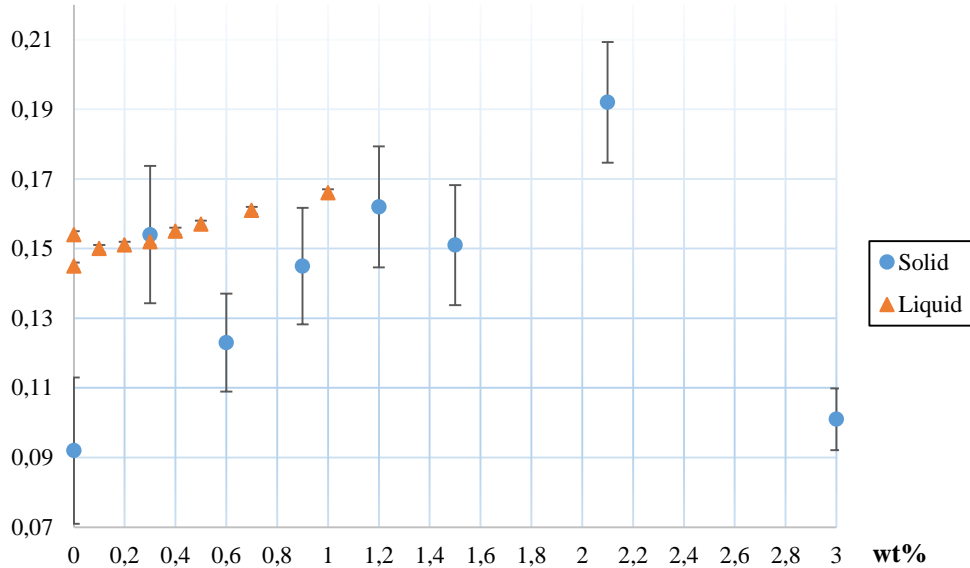


Figure 4.5 Comparison of  $\lambda_s$  and  $\lambda_l$  for CNTs.

There is a clear reduction of  $\lambda_s$  between 0,7 wt% and 1,0 wt% that should be justified examining some research showing that the addition of CNTs does not result in improvement of thermal conductivity, but in worsening. [43] This phenomenon is due to the fact that the carbon nanotubes have thermal conductivity greater than 3.000 W/mK if they are considered individually, but if they are considered as masses with mono or bi-dimensional distribution, the thermal conductivity decreases by 1 and 2 orders of magnitude respectively. While for a three-dimensional distribution are reached values lower than 0,2 W/mK, which is a typical value of thermal conductivity of an isotropic polymer. [44][43]

In Table 4.1 you can analyse the thermal conductivity ( $\lambda_s$ ) of three types of carbon nanotubes subjected to different pressures to increase the volume fraction ( $\phi$ ) and then to increase the contact surface between the nanotubes. It is well known that a large contact resistance limits the transfer of energy in the van der Waals contacts, due to weak intertube bonds. The contact resistance between the tubes decreases with increasing the size of the diameter of the nanotubes, due to a larger area of contact, even if nanotubes with smaller diameters should ensure a greater number of contacts intertube. The thermal resistance also depends on the length and the overlap of the nanotubes and the distances between the junctions. In fact, if the length is greater, if the overlap area of the nanotubes is bigger and if the distance between them is smaller, the intertube thermal resistance will be lower.[45] With the increase of the intertube space, the van der Waals interactions between the tubes

are weaken, reducing the heat that, among the nanotubes, may only be transmitted with this mechanism. Instead, when two nanotubes overlap and merge, the energy is transmitted through the bonds between the atoms, by improving the efficiency of heat transfer compared to the exchange mechanism with only van der Waals interactions. A greater length of the nanotubes is helpful to the increase of thermal conductivity, as it allows greater length overlaps and allows the transmission of heat through the molecular bonds for greater distances than those of shorter CNTs, exploiting less van der Waals intertube interactions, which have higher thermal resistance. [45]

**Table 4.1** Thermal conductivity of CNTs with different pressure. [43]

Sample	Pressure [psi]	$\lambda_s$ [W/mK]	$\phi$
<b>1-2 nm SWCNT</b>	20	0,155	17,2%
	50	0,175	18,1%
	90	0,194	19,4%
<b>&lt;8 nm MWCNT</b>	20	0,154	12,7%
	50	0,171	13,7%
	90	0,195	15,2%
<b>60-100 nm MWCNT</b>	20	0,134	8,9%
	50	0,154	10,4%
	90	0,170	12,4%

To add to these aspects, there is the transmission of heat at the interface between CNTs and the matrix, which likely influence the exchange of heat to the lack of functionalization. In fact, if there is a heat transfer problem between the nanotubes, the same problem may occur again in the interactions between the matrix and ENPs. To overcome this limit, it is necessary a functionalization of nanoparticles, which consists in adding a chemical functional group on the surface of the nanoparticle. This treatment has the purpose to obtain a surface modification that triggers an "automatic" organization and which render the nanoparticles compatible with the host material. The goal of functionalization is to coat the surface with a molecule having the appropriate chemical functionality for the desired application. [46] To carry out the functionalization is then necessary to identify the appropriate process for this purpose and the functional group that is chemically compatible with the nano-particle and with the matrix. The chemical compatibility is necessary to reduce the distance between the atoms and / or to generate the bonds between atoms of the nanoparticles and the matrix, while an automatic organization of ENPs allows to obtain a better and faster dispersion.

In this case the presence of agglomerates detectable to the touch and to the naked eye is an index of a not-optimal dispersion, which then influence the exchange of heat. In fact, these groupings are constituted by ENPs, which, randomly dispersed, possess a high thermal resistance in the tube-tube interactions. Moreover, the particle-matrix interface decreases, limiting the heat exchange.

Taking into account these phenomena, it is possible to justify the decrease of thermal conductivity with 1,0% of CNTs.

However, the main goal of this dissertation has been partially reached, in fact it was registered an enhancement of thermal conductivity adding CNTs both in liquid and solid phase, confirming the possibility of increasing the  $\lambda_s$  paint by adding small percentages of nanoparticles with high thermal conductivity. The main problem lies in the type of ENPs to be added, because it can greatly vary the aesthetic quality for the colour variations and the presence of agglomerates which vary the surface roughness when a good nano-dispersion is not obtained.

#### **4.4 Electrical conductivity**

The electrical behaviour of a nano-composite, after the addition of CNT, change from insulator to conductor, as soon as you establish at least one conductive path (percolation phenomenon), dependent on the concentration of nanoparticles (percolation threshold) between two opposite sides of the composite. The percolation threshold has been exceeded with 1,0 wt% of CNTs, in fact, CNT<sub>1,0%</sub> has electrical conductivity in alternating current ( $\sigma_{ac}$ ) about 4 orders of magnitude higher than that of Paint<sub>200%</sub>. The improvement in electrical conductivity was obtained also in the case of direct current ( $\sigma_{dc}$ ), but about 8 orders of magnitude.

This aspect can be considered a relevant factor in reducing the electrostatic charge of the non-conductive polymers. In fact, using chrome-plated plastics as an alternative to metals, the high electrical conductivity of the nanopaint prevents the possible electrostatic discharges when someone touches these elements.

#### **4.5 Health and environmental aspects**

The industrial-scale application of nanoparticles in many areas of daily life, as well as specific health applications, raises the question of the security of these systems. The nanometer size can give rise to concerns in relation to its small size, which could allow the crossing of natural barriers, resulting in

potential biological damage. In fact, the nanoparticles are much smaller than most known articulate matter PM<sub>10</sub>, (PM<sub>10</sub>, that is atmospheric particulate matter with a mean aerodynamic diameter of 10 µm) whose percentage in the atmosphere is used as an indicator of pollution. As has been seen, however, the nanoparticles term indicates diverse systems between them. Some nano-systems are used precisely in function of their biocompatibility, for use in diagnosis, replacing molecules used currently and whose toxicity is ascertained. Therefore, it makes little sense to worry generically of nanoparticles simply because of their size (many nanoparticles are produced spontaneously and are always present in the air we breathe or are unknowingly used for centuries). Their properties can depend on many details, the size, the exposed surface, the combination with other nano-systems, etc... and not only from the substance that constitutes them. It is therefore important to make sure that every new system and technology is subjected to focused experiments, in relation to the specific applications. If we process it, we must have a reasonable assurance that the specific nanoparticles used in paint is not harmful to people and the environment, compared to the expected exposure.



## 5 Conclusions and future work

### 5.1 Conclusions

The study carried out with nanoparticles of  $\text{Fe}_3\text{O}_4$  has not led us to the required solution, since it has failed on two important aspects. Firstly, the paint colour is significantly changed after the addition of nanoparticles and especially the brightness is decreased after the addition of low doses of less than 1 wt%. Second, the thermal conductivity measurements in the liquid phase have not given satisfactory results because they have not registered significant increases of  $\lambda_l$  compared to Paint<sub>200%</sub> (1,8% with 1,0 wt%). This has discarded the possibility of using such nano-additive for this type of nanopaint.

As regards the carbon nanotubes, best results were recorded for both the thermal conductivity in liquid phase and that one in the solid phase, with a peak of  $\lambda_s = 0,192 \pm 0,017 \text{ W/mK}$  for 0,7 wt% of CNTs, equal to an enhancement of 108,7% compared to Paint<sub>200%</sub>. However, despite these improvements, CNTs cannot be used for the purpose of this work because of the brightness variation already registered with 0,2 wt% of CNTs. Excessive reduction in brightness cannot be accepted as this feature is crucial to get a chrome effect and, with CNTs percentages higher than 0,2 wt%, the colour change is even more evident, tending to a matte dark grey.

About the procedure of mixing, painting and analysing, it will consist of the following steps:

- Preparation Paint<sub>200%</sub>: one part of base paint, two parts of diluent, mixed for 30 minutes with the magnetic stirrer
- Adding nanoparticles with mixing for at least 30 minutes with ultrasonic bath and manual mixing. There is the need to change the ultrasonic bath water every 10 minutes to prevent evaporation of the solvent
- Drawing up of the paint on the substrate for 4 times, every 10 minutes, to obtain a top layer to 25 pm, with final drying for at least one day
- Analysis to check for any changes in color using a spectrophotometer
- Removing the layer from the substrate to measure paint's thickness using an optical microscopy
- Obtaining of layer samples with dimensions  $3*3 \text{ cm}^2$  in order to measure the thermal conductivity with the Gustafsson Probe method
- Obtaining of layer samples with dimensions  $1*1 \text{ cm}^2$  to be able to measure the electrical conductivity with an electrometer

- Analysis of the results

## 5.2 Future work perspectives

The future work may be focused on two main aspects: the determination of the best nanoparticles to be added to the base paint and optimization of nano-dispersion.

As regards the nanoparticles most suitable for the purpose of the thesis, one must consider the thermal conductivity, the colour and the cost. There are various metals with high thermal conductivity, including gold, silver and copper (Table 5.1) to be taken as a reference for the choice of nanoparticles, but they are notoriously precious metals, therefore expensive, or in nano-metric dimensions they take colours that would affect too much the chrome effect (as for CNTs). Comparing the colours of different metals, commercially available in nano-powder, and selecting those with the best thermal conductivity, nano-aluminium particles (nano-Al) would be the best choice to continue this work. In fact, the grey colour of the nano-Al makes to presuppose that they do not significantly vary the colour of the base paint, leaving unchanged the chrome effect required. Furthermore, the thermal conductivity of aluminium is 290 W/mK, around 4 order of magnitude higher than that one of the base paint (0,092 W/mK).

**Table 5.1** Thermal conductivity of several materials.

Material	Thermal conductivity [W/mK]
Silver	460
Copper	390
Gold	320
Aluminium	290
Brass	111
Platinum	70
Steel	52
Lead	35
Stainless steel	17

As done for the CNTs in this work, even for nanopaint containing nano-Al will be necessary RGB analysis to assess changes in colour, thermal analysis in liquid and solid phases and electrical analysis to characterize the nanopaint.

Other tests are suggested for the evaluation of the quality of the nanopaint as the analysis of roughness and hardness of the layer after the addition of nanoparticles and a pull-off tests of the paint, which, according to other studies on paints, is supposed to show improvement after the addition of nanoparticles. [30] It is also recommend carrying out analyses with a thermographic camera to get photographic results that certify a possible improvement in the thermal conductivity. Functionalization of nanoparticles will be asked whether it will be necessary to optimize the nano-dispersion to avoid agglomeration for a higher surface quality and to get better percolation of ENPS that improves the thermal and electrical conductivity.



## 6 References

- [1] “Paint and Coatings Industry Overview - Chemical Economics Handbook (CEH) | IHS.” [Online]. Available: <https://www.ihs.com/products/paint-and-coatings-industry-chemical-economics-handbook.html>. [Accessed: 15-Oct-2015].
- [2] M. Amft, “Materials for the,” *Adv. Mater.*, 2005.
- [3] J. K. Dennis and T. E. Such, “Nickel and Chromium Plating”. 1993.
- [4] J. M. Tyler, “Automotive applications for chromium,” *Met. Finish.*, vol. 93, no. 10, pp. 11–14, 1995.
- [5] N. V. Mandich, “Practical problems in bright and hard chromium electroplating—Part I,” *Met. Finish.*, vol. 97, no. 6, pp. 100–112, 1999.
- [6] International Agency For Research on Cancer, “IARC Monographs on the Evaluation of Carcinogenic Risks to Humans,” *Iarc*, vol. 49, pp. 208–214, 1990.
- [7] A. Gambelunghe, R. Piccinini, M. Ambrogi, M. Villarini, M. Moretti, C. Marchetti, G. Abbritti, and G. Muzi, “Primary DNA damage in chrome-plating workers,” *Toxicology*, vol. 188, no. 2–3, pp. 187–195, 2003.
- [8] S. Roberti, T. Mabilia, C. F. Stocco, F. Sarto, and E. Merler, “Aumentata mortalità per tumori polmonari tra gli addetti a una cromatura a strato sottile An increased mortality from lung cancer among workers of a bright electroplating factory,” vol. 30, pp. 232–236, 2006.
- [9] P. Mohapatra, S. K. Samantaray, and K. Parida, “Photocatalytic reduction of hexavalent chromium in aqueous solution over sulphate modified titania,” *J. Photochem. Photobiol. A Chem.*, vol. 170, no. 2, pp. 189–194, 2005.
- [10] B. Navinsek, P. Panjan, and I. Milosev, “PVD coatings as an environmentally clean alternative to electroplating and electroless processes,” *Surf. Coatings Technol.*, vol. 116–119, pp. 476–487, 1999.
- [11] E. Bozyaz, M. Ürgen, and A. F. Çakr, “Comparison of reciprocating wear behaviour of electrolytic hard chrome and arc-PVD CrN coatings,” *Wear*, vol. 256, no. 7–8, pp. 832–839, 2004.
- [12] S. Kuroda, J. Kawakita, M. Watanabe, and H. Katanoda, “Warm spraying - a novel coating process based on high-velocity impact of solid particles,” *Sci. Technol. Adv. Mater.*, vol. 9, no. 3, p. 033002, 2008.
- [13] Thermo Fisher Scientific, “Chemical Compatibility Guide -The Chemical Resistance Chart,” *Chem. Resist. chart Resist.*, pp. 1–7.
- [14] “Processo di lavaggio.” [Online]. Available: <http://www.durr-ecoclean.com/it/prodotti/processo-di-lavaggio/>. [Accessed: 02-Mar-2016].
- [15] I. Pastorelli, “Verniciatura e controllo qualità. Proprietà, tecniche di lavorazione e controllo delle superfici vernicate”. HOEPLI EDITORE, 2004.
- [16] G. Bulla and L. Perbellini, “Le nuove tecniche di verniciatura e rischi per la salute,” *G. Ital. Med. Lav. Ergon.*, vol. 33, no. 3, pp. 257–263, 2011.

- [17] K. Krishnamoorthy, K. Jeyasubramanian, M. Premanathan, G. Subbiah, H. S. Shin, and S. J. Kim, "Graphene oxide nanopaint," *Carbon N. Y.*, vol. 72, pp. 328–337, Jun. 2014.
- [18] Umwelt Bundes Amt, "Use of Nanomaterials in Textiles," pp. 1–12, 2013.
- [19] T. G. Gutowski, J. Y. H. Liow, and D. P. Sekulic, "Minimum exergy requirements for the manufacturing of carbon nanotubes," *Proc. 2010 IEEE Int. Symp. Sustain. Syst. Technol. ISSST 2010*, 2010.
- [20] M. S. Selim, S. A. El-safty, M. A. El-sockary, A. I. Hashem, O. M. Abo, A. M. El-saeed, and N. A. Fatthallah, "Smart photo-induced silicone / TiO<sub>2</sub> nanocomposites with dominant [110] exposed surfaces for self-cleaning foul-release coatings of ship hulls," *JMADE*, vol. 101, pp. 218–225, 2016.
- [21] "product-characteristics" [Online]. Available: \
- [22] "linea-surfapore" [Online]. Available: <http://www.nanosilv.it>.
- [23] T. Xiao-zhou and W. Jian-fang, "Preparation and Properties of Fe<sub>3</sub>O<sub>4</sub> Biomimetic," vol. 3, no. 2, pp. 299–305, 2010.
- [24] a S. Khanna, "Nanotechnology in High Performance Paint Coatings," *Asian J. Exp. Sci.*, vol. 21, no. 2, pp. 25 – 32, 2008.
- [25] M. Rashvand, Z. Ranjbar, and S. Rastegar, "Nano zinc oxide as a UV-stabilizer for aromatic polyurethane coatings," *Prog. Org. Coatings*, vol. 71, no. 4, pp. 362–368, Aug. 2011.
- [26] Z. Wang, E. Han, F. Liu, and W. Ke, "Thermal Behavior of Nano-TiO<sub>2</sub> in Fire-Resistant Coating," vol. 23, no. 4, pp. 547–550, 2007.
- [27] H. E. Yong, K. Krishnamoorthy, K. T. Hyun, and S. J. Kim, "Preparation of ZnO nanopaint for marine antifouling applications," *J. Ind. Eng. Chem.*, vol. 29, pp. 39–42, 2015.
- [28] X. Zhang, F. Wang, and Y. Du, "Effect of nano-sized titanium powder addition on corrosion performance of epoxy coatings," *Surf. Coatings Technol.*, vol. 201, no. 16–17, pp. 7241–7245, May 2007.
- [29] Á. Yedra, G. Gutiérrez-somavilla, C. Manteca-martínez, M. González-barriuso, and L. Soriano, "Progress in Organic Coatings Conductive paints development through nanotechnology," *Prog. Org. Coatings*, vol. 95, pp. 85–90, 2016.
- [30] G. V. Pham, A. T. Trinh, T. Xuan, H. To, and T. D. Nguyen, "Incorporation of Fe<sub>3</sub>O<sub>4</sub> / CNTs nanocomposite in an epoxy coating for corrosion protection of carbon steel," vol. 035016, 2014.
- [31] T. Boon, N. Shariffa, F. Abas, H. Mirhosseini, I. Arbi, and C. Ping, "Comparing the formation of lutein nanodispersion prepared by using solvent displacement method and high-pressure valve homogenization : Effects of formulation parameters," *J. Food Eng.*, vol. 177, pp. 65–71, 2016.
- [32] J. F. U and A. Desrumaux, "Effect of high-pressure homogenization on droplet size distributions and rheological properties of model oil-in-water emulsions," pp. 127–134, 2000.
- [33] T. Hielscher, "Ens'05," no. December, pp. 14–16, 2005.
- [34] E. S. Bernhardt, B. P. Colman, M. F. Hochella, B. J. Cardinale, R. M. Nisbet, C. J. Richardson,

- and L. Yin, “An ecological perspective on nanomaterial impacts in the environment.,” *J. Environ. Qual.*, vol. 39, pp. 1954–1965, 2010.
- [35] U. of Essex, “Measurement Techniques For Nanoparticles,” pp. 1–7, 2014.
- [36] “Nanotechnology and the environment - Hazard potentials and risks.” [Online]. Available: <http://www.nanowerk.com/spotlight/spotid=25937.php>. [Accessed: 19-Nov-2015].
- [37] M. Simkó and A. Gazsó, “Nanosilver,” pp. 1–7, 2010.
- [38] K. Donaldson, R. Aitken, L. Tran, V. Stone, R. Duffin, G. Forrest, and A. Alexander, “Carbon nanotubes: A review of their properties in relation to pulmonary toxicology and workplace safety,” *Toxicol. Sci.*, vol. 92, no. 1, pp. 5–22, 2006.
- [39] M. Goldoni, A. Cagliari, D. Poli, M. V. Vettori, M. Corradi, P. Apostoli, and A. Mutti, “Determination of hexavalent chromium in exhaled breath condensate and environmental air among chrome plating workers.,” *Anal. Chim. Acta*, vol. 562, no. 2, pp. 229–235, Mar. 2006.
- [40] D. M. Mitrano, S. Motellier, S. Clavaguera, and B. Nowack, “Review of nanomaterial aging and transformations through the life cycle of nano-enhanced products,” *Environ. Int.*, vol. 77, pp. 132–147, 2015.
- [41] Amara L. Holder, Eric P. Vejerano, Xinzhe Zhou and Linsey C. Marr, “Environmental Science Processes & Impacts, Nanomaterial disposal by incineration” pp. 1652–1664, 2013.
- [42] “EasyRGB - The inimitable RGB and COLOR search engine!” [Online]. Available: <http://www.easycolor.com/index.php?X=CALC>. [Accessed: 08-Mar-2016].
- [43] R. S. Prasher, X. J. Hu, Y. Chalopin, N. Mingo, K. Lofgreen, S. Volz, F. Cleri, and P. Kebinski, “Turning Carbon Nanotubes from Exceptional Heat Conductors into Insulators,” vol. 105901, no. March, pp. 1–4, 2009.
- [44] J. Hone, M. C. Llaguno, N. M. Nemes, and A. T. Johnson, “Electrical and thermal transport properties of magnetically aligned single wall carbon nanotube films,” vol. 77, no. 5, pp. 666–668, 2000.
- [45] H. Zhong, “Interfacial Thermal Resistance Between Carbon Nanotubes : Molecular Dynamics Simulations and Analytical Thermal Modeling Interfacial Thermal Resistance Between Carbon Nanotubes : Molecular,” vol. 74, pp. 1–10, 2006.
- [46] R. Subbiah, M. Veerapandian, and K. S. Yun, “Nanoparticles : Functionalization and Multifunctional Applications in Biomedical Sciences Nanoparticles : Functionalization and Multifunctional Applications in Biomedical Sciences,” no. April 2016, 2010.